Marine Pollution Bulletin 201 (2024) 116191

Contents lists available at ScienceDirect

Marine Pollution Bulletin

journal homepage: www.elsevier.com/locate/marpolbul

Model-based estimation of seasonal transport of macro-plastics in a marine protected area

M. Stagnitti *, R.E. Musumeci

Department of Civil Engineering and Architecture, University of Catania, via S. Sofia 64, 95123 Catania, CT, Italy

ARTICLE INFO

Keywords:
Particle tracking model
Hydrodynamic simulation
River floods
Mediterranean Sea

ABSTRACT

Management of plastic litter in Marine Protected Areas (MPAs) is expensive but crucial to avoid harms to critical environments. In the present work, an open-source numerical modelling chain is proposed to estimate the seasonal pathways and fates of macro-plastics, and hence support the effective planning and implementation of sea and beach cleaning operations. The proposed approach is applied to the nearshore region that includes the MPA of Capo Milazzo (Italy). A sensitivity analysis on the influence of tides, wind, waves and river floods over the year indicates that seasonality only slightly affects the location and extension of the macro-plastic accumulation zones, and that beach cleaning operations should be performed in autumn. Instead, the influence of rivers on plastic litter distribution is crucial for the optimal planning of cleaning interventions in the coastal area.

1. Introduction

The issue of marine plastic litter has recently gained more attention, due to increasing records of plastics reported in different environmental matrices such as water, sediment, and biota as well as in drinking water and foods (Nunes et al., 2022). The so-called macro-plastics (i.e. single-use plastics or fragments with size above 25 mm) and meso-plastics (i.e. fragments with size between 5 mm and 25 mm), which are generally quite easy to see and remove from the environment, increase their bioavailability by breaking down into micro and nano-plastics (i.e. size below 5 mm and 1×10^{-4} mm, respectively), as a result of a variety of actions associated with UV radiation, mechanical transformations, and biological degradation processes (Thompson et al., 2004; Soares et al., 2020). Indeed, micro and nano-plastics derived from macro-plastic breaking, together with the so-called primary micro-plastics (e.g. micro-beads in cosmetics, plastic pellets) are ingested by animals which populate the sea, thus entering the food chain, and in the end hurting human health (Coppock et al., 2019; Claro et al., 2019; Shen et al., 2020). It is important to point out that micro and nano-plastics are likely to absorb and hence transport organic pollutants and other hazardous contaminants, because of their high surface area to volume ratio (Peng et al., 2020; Kiran et al., 2022).

In Europe, about 500,000 tons of plastic litter are released into the sea every year (Interreg Europe, 2021). Most plastic litter is produced inland by agricultural, industrial and urban activities, whose waste is transported by rivers towards the sea (Lebreton and Andrady, 2019). Moreover, the COVID-19 pandemic has led to an increased demand for single-use plastics (Alfonso et al., 2021; Al-Salem et al., 2022), which globally caused more than 25,000 tons of pandemic-associated plastic waste entering the global ocean, about 11 % of which is transported by European rivers (Peng et al., 2021). The Mediterranean Sea is particularly affected by the marine litter problem, not only because of the huge inland plastic waste production, but also due to the limited water exchanges with other oceans, to the intense offshore maritime traffic, and to the high temperatures accelerating plastic spreading into the environment (Fossi et al., 2020). On the one hand, the reduction of plastic waste entering the coastal environment should be pursued through the development of a greater environmental awareness based on education and dissemination of scientific knowledge (Soares et al., 2020), as well as through the implementation of circular economy management models. Such models are based on the so-called "3R", i.e. on the concepts of reduction, reuse and recycling (Wang et al., 2022), and they can be supported by a credit system (Lee, 2021). On the other hand, the removal of existing marine plastic litter through both beach cleanup and technologies operating on the water, e.g. booms and skimmers (Brouwer et al., 2023), should be effectively planned and implemented.

In order to legally bind measures to ensure Good Environmental Status (GES) in European marine waters, legislation and specific Regional Seas Conventions (RSCs) against plastic pollution have been developed, i.e. the Marine Strategy Framework Directive (MSFD, 2008/

* Corresponding author.
E-mail addresses: martina.stagnitti@unict.it (M. Stagnitti), rosaria.musumeci@unict.it (R.E. Musumeci).

https://doi.org/10.1016/j.marpolbul.2024.116191
Received 25 November 2023; Received in revised form 20 February 2024; Accepted 21 February 2024

56/EC) and the four RSCs OSPAR Commission for the North-East Atlantic region, HELCOM (Helsinki Commission - Baltic Marine Environment Protection Commission), Black Sea Commission (BSC), and UNEP/MAP Barcelona Convention for the Mediterranean Sea. The MSFD Technical Group on Marine Litter and the four RSCs pays specific attention to the plastic litter monitoring strategies, which are fundamental for the assessment of the current state of marine waters and of the risk related to plastic pollution, as well as of the effects of mitigation measures (González-Fernández and Hanke, 2020). In particular, standardized criteria for monitoring and sampling macro and micro-litter on the beach, the sea surface, the seafloor as well as in biota are provided, in terms of spatial distribution and timing of monitoring, size and material categorization of the samples, observation and sampling protocols, data reporting, required equipment, and costs. For the Mediterranean Sea, several local investigations have been carried out applying the MSFD and the UNEP/MAP criteria, with reference to beached (e.g. Poeta et al., 2016; Lots et al., 2017; Vlachogianni et al., 2018; Mandić et al., 2022), floating (Zeri et al., 2018; Campanale et al., 2019; Garcia-Garin et al., 2020; Galli et al., 2023), sea floor (e.g. Spedicato et al., 2019; Consoli et al., 2018; Saladié and Bustamante, 2021; Angiolillo et al., 2023) and biota (e.g. Alomar and Deudero, 2017; Valente et al., 2022) plastics.

The removal of existing marine plastic litter should be performed according to strategic and efficient intervention schemes based on the knowledge of its trajectories, destinations and fates (Critchell and Lambrechts, 2016; Van Sebille et al., 2020; Guerrini et al., 2021). Despite numerical modelling of the complex physical and biochemical processes that influence the transport of marine plastic litter still needs improvements (Liubartseva et al., 2018; Hinata et al., 2020), it represents the only existing tool for the prediction of the likely plastic pathways and the identification of possible accumulation zones, once the sources and quantities of released plastics are known. The simplest numerical models of marine plastic transport are based on the Lagrangian tracking of the particles due to winds, waves and currents (e.g. Isobe et al., 2009; Kako et al., 2014; Iwasaki et al., 2017; Rosas et al., 2022). Such an approach consists on the solution of the advection and diffusion equations for each released particle, for known values of drag and turbulence coefficients. The above-mentioned studies consider marine plastics to be neutral particles, neglecting washing-off and re-suspension phenomena, as well as degradation and biofouling processes. A more comprehensive representation of all the phenomena influencing marine plastic transport is provided by the so-called hydrodynamic and process-based models (Uzun et al., 2022), which combine the traditional Lagrangian tracking with more or less sophisticated formulations describing biological and physical effects on particle behavior. For instance, some advanced Lagrangian particle tracking models include a module to simulate the beaching phenomena, based on the identification of those particles that reach the land domain (e.g. Delandmeter and Van Sebille, 2019; Macias et al., 2019; Cardoso and Caldeira, 2021; Dobler et al., 2022; Castro-Rosero et al., 2023), eventually including washing-off processes through site-specific formulations (e.g. Wisha et al., 2022) or more sophisticated probabilistic approaches (e.g. Alosairi et al., 2020; Sousa et al., 2021; Onink et al., 2022). With reference to the degradation processes from macro to micro-plastic, Chassignet et al. (2021) combined the model Parcels v2.0 (Delandmeter and Van Sebille, 2019) with a simple, hypothetical exponential decay function for the weight of the particles. Also the Second-generation Louvain-la-Neuve Ice-ocean Model (SLIM; www.climate.be/slim) employed by Critchell and Lambrechts (2016) is able to take into account beaching, settling, re-suspension/re-floating, degradation into micro-plastics and topographic effects on the wind in nearshore waters. Similarly, Liubartseva et al. (2018) proposed a 2D Lagrangian model integrated with algorithms of beaching and sedimentation of plastics to be solved using a Monte Carlo technique. Jalón-Rojas et al. (2019) introduced the 3D numerical model TrackMPD, which is able to include also the effects of the biofouling process on the micro-plastic buoyancy, using as representative parameters the biofilm thickness, density and growth rate. Instead, Tsiaras et al. (2021) modeled the increase of micro-plastic density due to biofouling through a simplified estimation of the biofilm growth as a function of bacterial abundance. Further studies on micro-plastics behavior are still needed to enable the numerical simulation of other processes, such as hetero- and homo-aggregation, agglomeration, weathering and photodegradation (Bigdeli et al., 2022).

The issue of plastic litter pollution is particularly challenging for Marine Protected Areas (MPAs) (Wang et al., 2023). MPAs are meant to preserve local biodiversity and support the growth and conservation of marine animal and plant species, thus ensuring the protection of natural habitats from the impacts of human activities (Balbar and Metaxas, 2019). Due to their importance, MPA represent the majority of protected areas that cover almost 21 million km^2 and have been established worldwide since 2010 (UNEP-WCMC and IUCN, 2021). Nowadays, the strategic management of MPAs is mainly based on the maintenance of ecosystem services (Maestro et al., 2019), also considering the need for resilient responses to the effects of climate change (Wilson et al., 2020). However, biodiversity of MPAs is threatened by environmental contamination due to toxic organic chemicals and plastic waste.

In the present paper, a numerical investigation on marine plastic litter transport in the coastal region that includes the MPA of Capo Milazzo (Italy) is presented. The aim of the work is to propose an open-source modelling chain to quantify the effects of seasonality on marine plastic transport in coastal areas and derive useful information for the management of cleaning operation in the study area. Moreover, the work contributes to the scarce state-of-art on the numerical modelling of marine litter trajectories and fates in coastal regions. Indeed, research mainly focused on the modelling of global oceans (e.g. Chassignet et al., 2021; Klink et al., 2022; Li et al., 2023), open seas (e.g. Kako et al., 2014; Critchell and Lambrechts, 2016; Iwasaki et al., 2017; Cardoso and Caldeira, 2021; Allison et al., 2022), enclosed seas (e.g. Carlson et al., 2017; Liubartseva et al., 2018; Li et al., 2018; Baudena et al., 2022; Murawski et al., 2022), and gulfs (e.g. Alosairi et al., 2020; Zayen et al., 2020). To the authors' knowledge, only few numerical investigations have been carried out for coastal waters, and in particular for estuaries (Sousa et al., 2021; Cloux et al., 2022; Pilechi et al., 2022), lagoon systems (Cardoso-Mohedano et al., 2023), small bays (Wisha et al., 2022), and narrow straits (Tong et al., 2021).

Since micro-plastics spreading throughout the sea originate from land-coming macro-plastics, here we focus on circulation patterns to identify locations where early removal, before offshore dispersion, would be strategic to mitigate the overall marine and coastal plastic contamination risk (Cloux et al., 2022). Therefore, a coupled hydrodynamic and Lagrangian particle tracking model is employed, to simulate the transport of buoyant and non-buoyant macro-plastics in the coastal area, including the beaching and washing-off processes, and considering the effects of seasonal circulation due to the combination of tide, waves and wind, which represent the main contributors to the plastic transport on the inner marine shelf (Alsina et al., 2020; Feng et al., 2022; Passalacqua et al., 2023), as well as the influence of river floods. The position of the release points and the physical and chemical characteristics of macro-plastics are derived from the outcomes of a field survey and of the laboratory analysis of collected plastic samples. The results of the numerical simulations provide insights on the plastic pathways and possible accumulation zone, which give fundamental indications for the optimal planning of removal interventions.

2. Materials and methods

2.1. Marine Protected Area of Capo Milazzo

The MPA of Capo Milazzo, which was established on March 2019 and hosts a variety of landscapes, cliffs and beaches of great environmental and panoramic value, is located in North-Eastern Sicily, in the middle of the Mediterranean Sea (Fig. 1a). The Mediterranean Sea is a very sensitive and vulnerable area (Interreg Europe, 2021), and retains most of

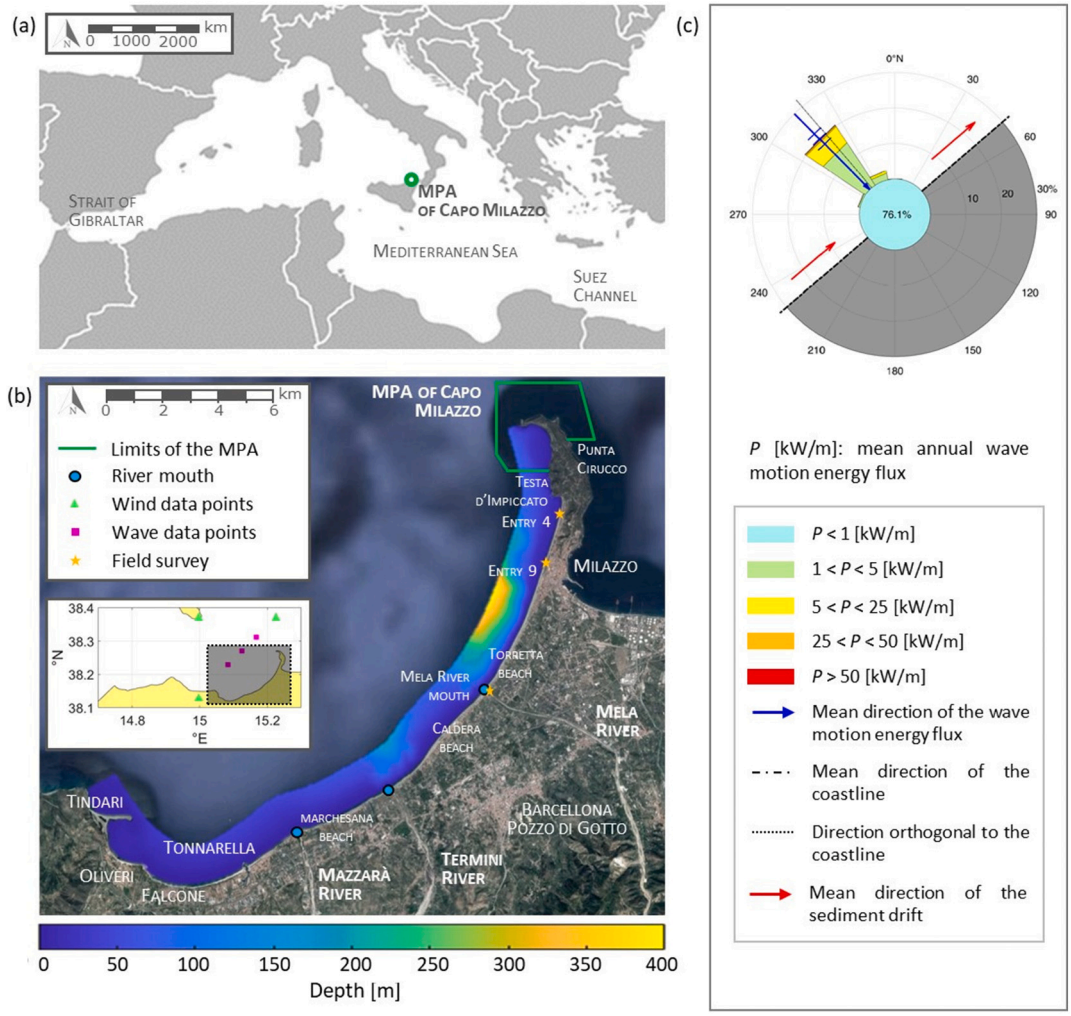

Fig. 1. Characterization of the study area: (a) geographic location of the MPA of Capo Milazzo; (b) satellite view (Google Earth, 2022) and the bathymetry of the study area, with indication of the wind and wave data points (coordinate system WGS84), of the main towns and rivers, and of the places of the field survey; (c) data on sediment drift derived from PRCEC (2020).

the released plastic waste because of its almost closed nature (Fossi et al., 2020; Baudena et al., 2022). As shown in Fig. 1b, the study area belongs to the about 30 km-long physiographic unit between Tindari and Capo Milazzo, which is characterized by fine gravel beaches, with the exception of the rocky coast of Capo Milazzo. The MPA encloses the Capo Milazzo promontory and the two adjacent areas which include the shallow beach that winds towards West up to Testa d'Impiccato, and the rocky coast of the Eastern sector up to Punta Cirucco (Fig. 1b). The fine gravel beach South of the MPA is about 26 km long, with a constant emerged slope of about 10 % and a variable cross-shore extent in the following ranges: 45÷70 m between the MPA and the Termini river, 30÷50 m between the Termini and Mazzarà rivers, 15÷35 m between the Mazzarà river and the town of Tonnarella, 20÷40 m between the towns of Tonnarella and Tindari. The Eastern stretch of coast is characterized by the presence of some rubble-mound breakwaters and groins for coastal protection. The bathymetry of the study area is shown in Fig. 1b.

The vulnerability of the MPA to plastic pollution is likely to be mainly connected to the intense inland urbanization and to the local touristic activities. Indeed, the results of several field campaign revealed that the percentage of beached (Prevenios et al., 2018; Vlachogianni et al., 2018; Asensio-Montesinos et al., 2021; Corbau et al., 2023), floating (Campana et al., 2018) and seafloor (Saladié and Bustamante, 2021; Scotti et al., 2021) plastics in the Mediterranean Sea coming from shoreline sources, mismanaged waste on land, and tourism-recreation activities reaches values up to 62 %, 23 % and 66 %, respectively. More specifically, the analysis of sea floor litter collected during the years 2011–2019 in the area between the MPA of Capo Milazzo and the Eolian Islands presented by Scotti et al. (2021) shows that 60 % of the sea floor plastics comes from the above-mentioned sources, whereas the remaining 40 % is equally distributed among fishing and aquaculture, sanitary and sewage related sources, fly-tipping, and shipping. Such results are in accordance with the outcomes of the monitoring activities of the INTERREG Med Plastic Busters MPAs project carried out in the period 2020–2021 (Argyropoulou and Papaioannou, 2022; ISPRA et al., 2022). Shoreline, tourism and recreational activities are found to produce from 25 % to 82 % of beach macro-litter of the MPA of Capo Milazzo. Moreover, fly-tipping, fishing and aquaculture, and sanitary and sewage related sources generate no more than 18 %, 14 % and 10 % of the observed beach macro-litter, respectively. Finally, the combination of shipping, agricultural waste and medical waste is responsible of less than 10 % of the observed beach macro-litter. Also numerical studies demonstrate that most of the plastic pollution of almost every Mediterranean country's coastline is caused by its own terrestrial sources of plastics (Liubartseva et al., 2018), with about 30 % to 55 % of all particles likely arriving at the coast after traveling less than 30 km (Macias et al., 2022). In particular, the Milazzo plain is densely urbanized. There are productive activities linked to the citrus, horticultural

and agropastoral traditions, as well as a complex mobility hub represented by the Port of Milazzo, by important refineries, and by the local railway and motorway nodes. Furthermore, the gravel beaches between Tindari and Capo Milazzo are a major tourist attraction thanks to their considerable extension, water quality and valuable landscape, housing several tourist facilities. Finally, a small harbor has been constructed in the area near Tonnarella (Fig. 1b).

Plastic waste produced by the above-mentioned activities can be directly thrown into the sea, or transported from the inland areas by rivers. The mouths of three rivers, namely Mazzarà, Termini and Mela rivers, are located in the study area South of the MPA (Fig. 1b). As described by the "Piano per l'Assetto Idrogeologico - P.A.I." (i.e. a plan to manage hydrogeological and hydraulic risk) of the Sicilian Water District Authority, the three corresponding watersheds, which are broad-leave-shaped, are characterized by a rugged morphology, with narrow valleys having steep slopes, deeply engraved by short thalwegs with significant bed slope, alternating with mountainous elevations which often reach heights greater than 1000 m above mean sea level (P.A.I., 2004a, 2004b, 2004c). Table 1 reports some geomorphological characteristics of the three watersheds, namely the surface area (A), the length and the mean bed slope of the main reach (L and i, respectively), the concentration time (t_c) calculated using the Kirpich (1940) formula, and the runoff coefficient (C), which depends on the soil morphology, the slope of the main river and the land use according to the indication of the Frevert table (Diaconu and Şerban, 1994). Moreover, the number of towns located inside each watershed and the corresponding number of residents are also provided.

The pluviometric regime characteristic of the three watersheds is described by the following rainfall depth-duration-frequency (DDF) curve:

$$h = at^b \tag{1}$$

where h is the rainfall depth, t is the rainfall duration, and a and b, which vary with the return period (T_r), are the empirical coefficients calibrated on the hourly rainfall data acquired during the years 1959–2004 by the Milazzo station of the rain gauges network managed by the Water Observatory of the Sicilian Region. The widely used rational method allows the estimation of the peak flow rates Q_{p,T_r} corresponding to the return period T_r for each of the three watersheds:

$$Q_{p,T_r} = \frac{C \cdot h_{T_r}(t_c) \cdot A}{t_c \cdot 3.6} \tag{2}$$

where $h_{T_r}(t_c)$ is the rainfall with duration equal to t_c for the return period T_r calculated through Eq. 1, and C and A are the watershed Frevert runoff coefficient and surface, respectively (Table 1). Table 2 reports the empirical coefficients of the rainfall DDF curve and the corresponding peak flow rates for T_r equal to 2, 50 and 100 years.

When plastic litter is released into the sea, whether directly or by the rivers, it spreads according to the local hydrodynamic circulation patterns, which may cause large sea surface plastic concentration, as demonstrated by the numerical investigation of Liubartseva et al. (2018). As shown in Fig. 1c, the mean direction of the sediment drift estimated from the analysis of the mean annual wave motion energy is about 50°N (PRCEC, 2020), right towards the MPA. Therefore, the MPA appears seriously threatened by plastic flows coming from South-West.

Table 2
Coefficients of the rainfall depth-duration-frequency (DDF) curves calculated for the study area and corresponding peak flow rates estimated by applying the rational method.

T_r [years]	a [mm/h]	b [−]	Q_{p,T_r} [m^3/s]		
			Mazzarà river	Termini river	Mela river
2	28.4	0.246	237.7	230.5	123.4
50	66.2	0.189	525.2	507.1	271.6
100	74.0	0.181	583.5	563.0	301.6

2.2. Wind, wave and sea level data

Time series of wind, wave and sea level are required to characterize the local wind and hydrodynamic conditions. As regards wind, the reanalysis dataset ERA5 from 1979 to the present day (Hersbach et al., 2018) is employed. Such a dataset, which is characterized by temporal resolution of one hour and spatial resolution of about 30 km, contains a huge number of global climate descriptors, including components of wind velocity at an elevation of 10 m above sea level. Among the available grid points, the ones with coordinates 38.3710°N - 15.2327°E, 38.3710°N - 14.9827°E, and 38.1210°N - 14.9827°E are the closest to the study area (Fig. 1b).

The characterization of the local offshore wave climate is based on the reanalysis dataset MEDSEA_ MULTIYEAR_ WAV_ 006_ 012 (Korres et al., 2021), which covers the period from 1993 to present day. The dataset is composed by time series of several wave descriptors, such as significant wave height (H_s), peak wave period (T_p) and mean wave direction (D_m), with temporal resolution of one hour and spatial resolution of 4 km along the WE direction and 5 km along the NS direction. For the site of interest, three offshore grid points are considered (Fig. 1b), namely point 1 (latitude: 38.2292°N; longitude: 15.0833°E; depth: 400 m), point 2 (latitude: 38.2708°N; longitude: 15.1250°E; depth: 600 m) and point 3 (latitude: 38.3125°N; longitude: 15.1667°E; depth: 800 m), in order to propagate wave data up to 20 m water depths through a SWAN simulation, thus obtaining a horizontal spatial resolution close to the coast of about 250 m.

Finally, sea level variations due to astronomical tides is calculated using the harmonic components provided by the Italian National Sea Monitoring Network for the Strombolicchio station (latitude: 38.8174°N; longitude: 15.2516°E).

2.3. Field survey

A field survey was performed on the 15th of February 2022, in order to acquire information on the polymer types mainly present in the study area. This analysis has been useful for the characterization of the plastic particles in the tracking model described in Section 2.4.2. Since the study area appears quite homogeneous in terms of beach morphology, climate forcing and land use, the stretch of coast between the MPA of Capo Milazzo and the Mela river mouth was selected as representative of the entire area. In particular, the following locations were visited (Fig. 1b): i) stretch of coast near the beach entry 4; ii) stretch of coast near the beach entry 9; iii) area of the Mela river mouth.

During the field survey, 22 plastic samples were collected and several pictures of beach litter were taken. The sampling methodology, which is

Table 1
Characteristic parameters of the watersheds located inside the study area (A = watershed surface area; L = length of the main river; i = mean bed slope of the main river; t_c = time of concentration; C = Frevert runoff coefficient). Data elaborated from (P.A.I., 2004a, 2004b, 2004c).

Watershed	Geomorphology				Demography		
	A [km^2]	L [km]	i [%]	t_c [hours]	C	No. of towns	No. of residents
Mazzarà	119.23	24.54	4.91	2.48	0.50	10	25,795
Termini	102.2	26.00	4.50	2.68	0.60	6	115,080
Mela	64.97	24.62	4.18	2.64	0.50	9	96,237

inspired by the European guidelines (European Commission, 2013), consists in the following steps: i) identification of a W-wide stretch of the beach; ii) partition of such a stretch in zones (Fig. 2), namely dune/backshore (D), central beach (C) and swash zone (S); iii) collection of representative macro-plastic samples, with dimensions not lower than 0.02 m. Each collected sample is identified by a code containing information about the beach entry, the stretch of coast and the zone of the beach where it was picked up. The mentioned information relative to the geometrical characteristics of the stretch of coast and to the identification of the plastic samples were reported in on-purpose designed datasheets, together with notes of the operators. The collection of plastics was based on a preliminary visual inspection of each zone of the visited stretch of coast, which allowed the identification of the representative items found on the considered portion of beach.

Table 3 reports the characteristics of the beach stretches where the samples were collected. For entry 4, two adjacent stretches were considered, both 20 m wide. Instead, for entry 9 three adjacent stretches were chosen, the first two 20 m wide and the third one 150 m wide. The Mela river mouth cannot be characterized by the quantities W, D, C and S employed for the beach stretches. It should be noted that all the considered stretches of beach are characterized by sediments with diameter (d) between 2 and 10 mm, belonging to the class of gravels. The summary of the samples is presented in Table 4, where the beach entry, stretch and zone where they were collected are indicated. Moreover, for each sample a brief description is provided. For instance, Fig. 2 shows the plastic samples collected in the stretch of coast no. 1 of the entry 4.

Although the field survey was not specifically performed to assess plastic litter sources, it provided useful insights for their characterization. The typology of litter observed in the study area, which was mainly made up by plastic bottles and caps, envelopes, and remains of beach equipment (e.g. slippers, balls, fragments of beach furniture), is coherent with the main plastic sources identified by Scotti et al. (2021) and by the monitoring activities of the INTERREG Med Plastic Busters MPAs project (Argyropoulou and Papaioannou, 2022; ISPRA et al., 2022), i.e. shoreline sources including mismanaged waste on land, and tourism-recreation activities and beachgoers. Moreover, the huge amount of plastic litter observed at the Mela river mouth confirmed that it is a plastic inlet. Finally, during the field survey a poorly managed landfill was found in the backshore near the Mela river mouth, from which plastic fragments can be moved by wind, rain water run-off or sea storms, thus crossing the protection fence and reaching the sea.

As briefly shown in Fig. 3a, no plastics were found in the central beach zone. About 60 % of the collected plastics was accumulated in the backshore, whereas the remaining part were picked up in the swash zone. Considering that beach cleaning operation are not performed during the winter season in the study area, the observed spatial distribution of beach litter was produced only by natural forcing. Although wind can certainly relocate items on the beach, it seems not realistic that a single wind gust has homogeneously leveled about 7 km of beach and pushed all the litter, including relatively heavy objects and wood debris, towards the backshore. Instead, this was more likely due to the action of sea storms occurred during the period antecedent to the field survey. Indeed, intense storm events typical of winter and autumn seasons can be an important driver of marine litter and natural wrack accumulation (Menicagli et al., 2022). The analysis of the time series of significant wave height relative to point 2 (Section 2.2) revealed that a total of 14 minor and major storms occurred between December 2021 and the date of the field survey, with peak significant wave height up to 4.15 m. The observations concerned only the surface of the beach, thus we cannot exclude that buried plastics could be present in the lower layers of the beach material. The Mela river was dry when the field survey was performed, and hence the presence of a concentration of plastic waste was observed in the area of the mouth. It is worth to point out that samples were collected only on the banks of the mouth, as the central area was not accessible.

Specific laboratory analyses were performed to determine the polymer type and densities of the collected plastic samples. The results reveal that PP (polypropilene), PET (polyethylene terephthalate) and HDPE (high-density polyethylene) represent the larger portion of collected plastics (Fig. 3b), with density (ρ) values ranging from 0.9 to 1.4 g/cm^3

Table 3
Characterization of the stretches of coast where the plastic samples have been collected (W = longshore width of the stretch of coast, D = cross-shore width of the backshore, C = cross-shore width of the central beach, S = cross-shore width of the swash zone, d = diameter of the sediments).

Site	Stretch	W [m]	D [m]	C [m]	S [m]	Beach sediments
Entry 4	1	20.00	15.00	29.00	6.00	Gravels
	2	20.00	15.00	29.00	6.00	($d = 2 \div 10$ mm)
	3	20.00	6.40	38.00	5.60	
Entry 9	4	20.00	6.40	38.00	5.60	Gravels
	5	20.00	6.40	38.00	5.60	($d = 2 \div 10$ mm)
	6	150.00	6.40	38.00	5.60	
Mela river mouth	–	–	–	–	–	Gravels ($d = 2 \div 10$ mm)

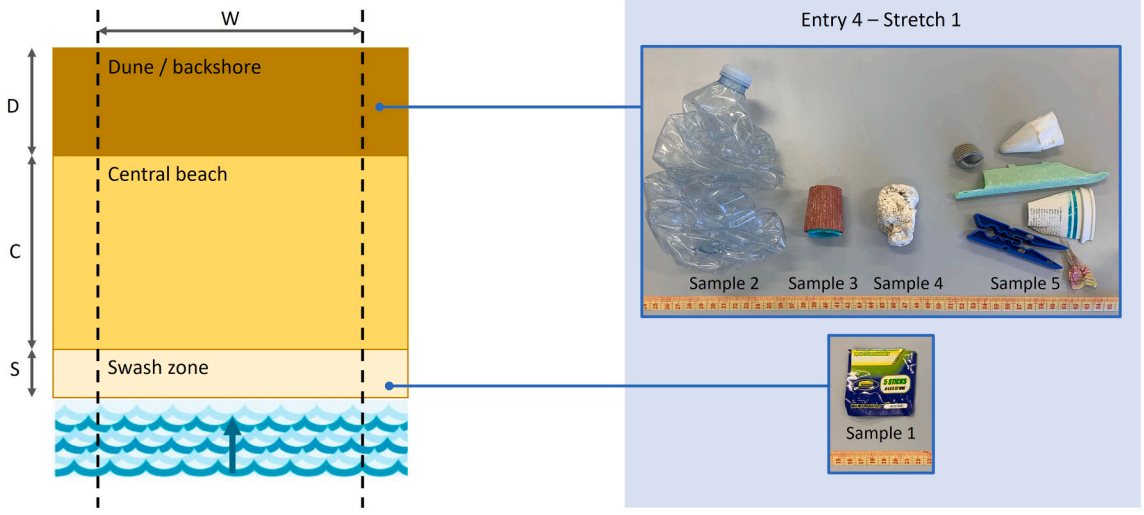

Fig. 2. Sketch of the partition of a generic stretch of beach employed for the collection and classification of the plastic samples. Examples of collected plastic samples are also shown.

Table 4
Summary of the collected plastic samples, with indication of materials (HDPE = high-density polyethylene; LDPE = low-density polyethylene; PET = polyethylene terephthalate; PLA = polylactic Acid; PMMA = polymethyl methacrylate; PP = polypropylene; PS = polystyrene) and densities (ρ).

Site	Stretch	Sample	Zone of the beach	Description	Polymer	ρ [g/cm^3]
Entry 4	1	1	S	Little envelope	PP	0.92
		2	D	Bottle	PET	1.35
		3	D	Double layer cap	PP	0.93
		4	D	Irregular piece	PS	1.02
		5	D	Various fragments	PP	0.93
	2	1	S	Irregular piece	PP	0.93
	3	1	D	Irregular piece	HDPE	0.95
Entry 9	4	1	D	Various fragments	HDPE	0.95
		2	S	Irregular piece	HDPE	0.95
	5	1	S	Irregular piece	PMMA	1.19
	6	1	S	Bottle	PET	1.35
		2	D	Fragment of black bag	LDPE	0.91
River Mela mouth	–	1	–	Irregular piece	HDPE	0.95
		2	–	Irregular piece	HDPE	0.95
		3	–	Irregular piece	PLA	1.25
		4	–	Irregular piece	PP	0.93
		5	–	Irregular piece	LDPE	0.91
		6	–	Irregular piece	HDPE	0.95
		7	–	Irregular piece	PS	1.02
		8	–	Irregular piece	PP	0.93
		9	–	Bottle	PET	1.35
		10	–	Bottle	HDPE	0.95

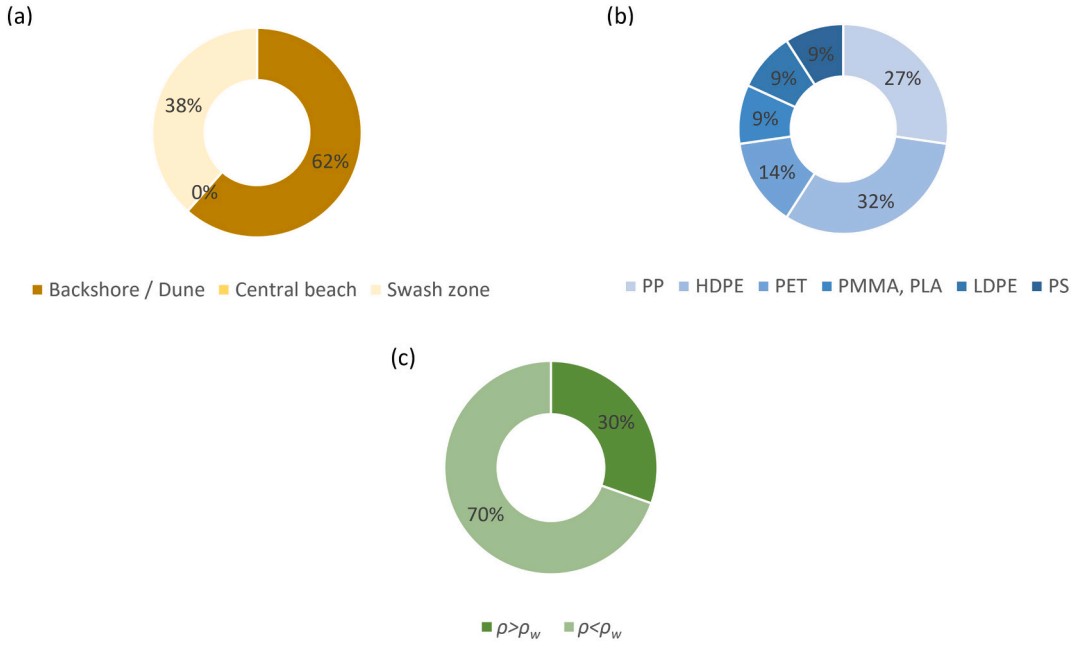

Fig. 3. Laboratory characterization of the collected plastic samples: (a) spatial distribution along the beach cross-section (the samples collected in the vicinity of the Mela river mouth are excluded); (b) constituent polymers; (c) percentage of collected samples with density higher or lower than the water density.

(Table 4). Fig. 3c shows that the collected plastics are mainly non-floating objects, being ρ of the 70 % of the samples higher than the water density ρ_w.

2.4. Numerical modelling

Three-dimensional numerical simulations of macro-plastic transport in the coastal area adjacent to the MPA of Capo Milazzo are performed by combing the hydrodynamic model Delft3D Flexible Mesh (Deltares, 2021a, 2021b) and the particle tracking model TrackMPD (Jalón-Rojas et al., 2019). In the following, a brief description of the employed numerical models and of the simulated scenarios is provided.

2.4.1. Hydrodynamic model

The hydrodynamic circulation in the study area is simulated by using the open source software Delft3D Flexible Mesh, which is able to carry out simulations of hydrodynamic flow, waves, water quality and ecology. The Delft3D Flexible Mesh Suite is composed of several modules, grouped around a mutual interface, while being capable to interact with one another. In the present work, the D-Flow FM and D-Waves modules are employed through an online coupling, in order to create an integrated model able to simulate the currents induced by both winds, sea level variations, and wave energy fluxes.

The module D-Flow FM (Deltares, 2021a) solves the two-dimensional (2DH, depth-averaged) or three-dimensional (3D) unsteady shallow water equations, which consist of the horizontal equations of motion, the continuity equation, and the transport equations for

conservative constituents. In the present work, a depth-averaged approach is employed because the fluid can be assumed vertically homogeneous. The choice of a 2D depth-averaged hydrodynamic model is in accordance with the state of the art on numerical modelling of nearshore circulation (Nielsen, 1992; Svendsen, 2005), as it allows the reduction of the computational times without significant loss of the physics. The unsteady shallow water equations are solved for unstructured calculation grids, under the Boussinesq assumptions, which are derived from the three-dimensional Navier-Stokes equations for incompressible free surface flow. The flow can be forced by tide at the open boundaries, wind stress at the free surface, pressure gradients due to free surface gradients or density gradients. Source and sink terms are included in the equations to model the discharge and withdrawal of water. The effects of surface waves on the flow are modeled by including wave forcing through radiation stress gradients, Stokes drift and mass flux, derived from the outputs of the D-Waves module (Deltares, 2021b), which is based on the third-generation spectral model SWAN (Booij et al., 1999).

Fig. 4 shows the numerical domain used in the present work. Such a domain follows the shape of the coast, which is about 30 km long, expanding towards offshore by about 1.20 km, thus covering an area of 37 km^2. The domain includes water depths between 0 and 400 m. The calculation grid, constructed using the RGFGRID software (Deltares, 2021c), contains 66,296 rectangular cells, whose size decreases along the onshore direction. In particular, the cell size in the longshore and onshore directions ranges between 14÷70 m and 7÷45 m, respectively. The choice to use a variable cell size allows us to ensure a high resolution at the lower water depths (see the bathymetry in Fig. 4), also minimizing computational costs. The time step during the simulations is dynamically adjusted ensuring a Courant number not higher than 0.7, and the temporal resolution of the simulation outputs is one hour. Using a processor Intel Core i7–9700 3.00 GHz, five days are simulated in 1÷2 h, depending on the open boundary condition and external forcing.

Open boundary conditions and other forcing have to be set, in order to induce the generation of the currents. Fig. 4 shows the location of the open boundaries for the employed numerical domain. In the D-Flow FM module, the lateral and offshore boundaries are forced by the astronomical tide, whose signal is calculated through the harmonic components. A constant and uniform wind field whose characteristics are derived from the analysis of the dataset ERA5 (Section 2.2) is set, in terms of wind velocity and direction. The river floods are included by specifying the discharge time series. For the present model, constant river discharges are considered.

As regards the wave boundary conditions, they are set in the D-Waves module at the offshore boundary. A Jonswap spectrum with peak enhancement factor equal to 3.3 is employed to characterize the wave forcing. For 11 almost equally spaced points (spatial step of about 3 km) located along the offshore boundary (Fig. 4), the following wave parameters are extracted by analyzing propagated waves at 20 m water depths (Section 2.2): H_s, T_p, D_m, and the directional spreading factor.

2.4.2. Particle tracking model

Transport and fates of macro-plastics are simulated through the TrackMPD model (Jalón-Rojas et al., 2019), using as hydrodynamic input the outcomes of the coupled D-Flow FM and D-Waves modules, which are properly processed to ensure compatibility between the two numerical models. TrackMPD is a three-dimensional particle-tracking model for the transport of marine plastic debris in oceans and coastal systems, which extends the traditional Lagrangian modelling of advection and diffusion processes by adding more-complex and realistic particle behaviors and physical processes, i.e. particle beaching and washing-off, sinking and deposition, windage, degradation from macro to micro-plastics, and biofouling growth on micro-plastics surface.

The three-dimensional particle displacement $\mathbf{dX} = (dX, dY, dZ)$ is calculated by solving the following vectorial equation:

$$\mathbf{dX}(t) = \mathbf{dX_{adv}}(t) + \mathbf{dX_{diff}}(t) + \mathbf{dX_{sink}}(t) = \mathbf{U}(x, y, z, t)dt + \mathbf{dX}'(t) + \mathbf{dX_{sink}}(t) \quad (3)$$

where the advective displacement $\mathbf{dX_{adv}} = (dX_{adv}, dY_{adv}, dZ_{adv})$ is given by the Eulerian velocity field $\mathbf{U} = (u, v, w)$ provided by the hydrodynamic model, the turbulent diffusion term $\mathbf{dX_{diff}} = (dX_{diff}, dY_{diff}, dZ_{diff})$ at the scale of the particle motion is reproduced by a random component $\mathbf{dX}' = (dX', dY', dY')$, and the sinking displacement $\mathbf{dX_{sink}} = (0, 0, -w_s dt)$

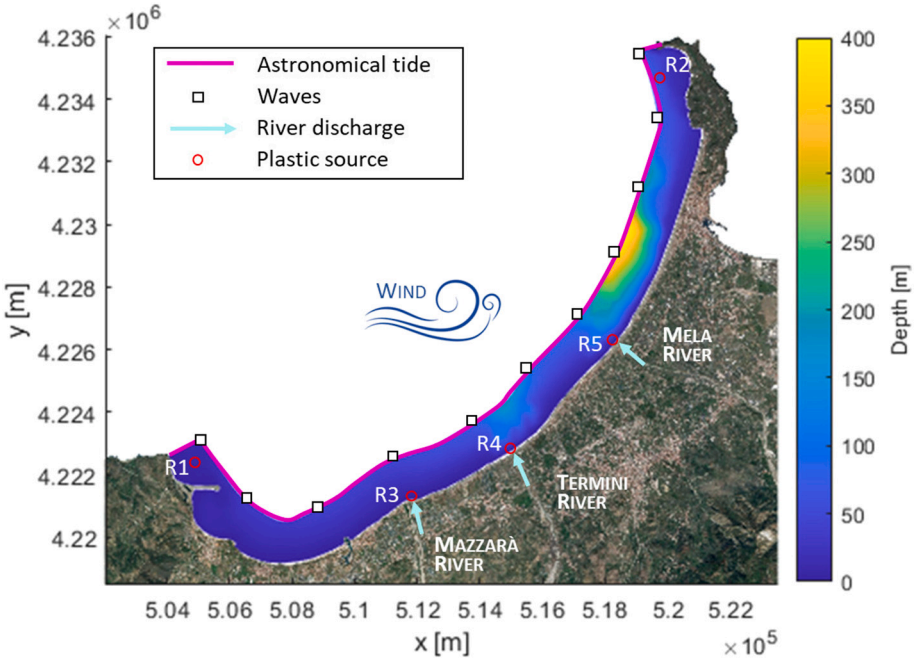

Fig. 4. Numerical domain used to model the marine plastic transport in the study area, with representation of the bathymetry, definition of the boundary conditions and forcing employed in the hydrodynamic model, and indication of the plastic sources set for the particle tracking simulations (coordinate system WGS84 UTM zone 33 N).

depends on the settling velocity of the particles $w_s(t)$.

The numerical solution of Eq. 3 requires the identification of the grid cells in which each particle is located and the subsequent interpolation of the water properties, such as current velocity, sea surface height and horizontal and vertical diffusivities. Then, a Runge-Kutta scheme of order 4/5 in both space and time is used to calculate the term $\mathbf{dX_{adv}}$ of Eq. 3, whereas a random-walk model is used to simulate the turbulent particle motion $\mathbf{dX_{diff}}$ as a function of horizontal and vertical diffusivities (K_h and K_v, respectively). As regards the term $\mathbf{dX_{sink}}$, the settling velocity w_s can be set by the user or calculated by TrackMPD according to the particle physical properties (i.e. particle density, shape and size), including the effects of biofouling and degradation processes.

About beaching and washing-off processes, a particle that has reached the land is considered beached, and it can be washed-off only by high tide. In particular, particles at high tide are washed-off with a probability P calculated through a Monte Carlo approach as follows:

$$P = 0.5^{-t/T_w} \tag{4}$$

where t is the time step from the last beaching and T_w is the half-life for debris to remain on the beach before being washed-off again. Beached particles are washed-off from the coast at high tides if a randomly generated number between 0 and 1 is lower than the calculated P.

In the present work, 3D trajectories are computed considering that $\mathbf{U} = (u, v, w)$ is a depth-uniform 2D velocity field, where w is considered null. Therefore, dZ_{adv} and dZ_{diff} in Eq. 3 are null, and the particle displacement along the z direction is calculated considering only the contribution of the particle settling velocity, without possibility to refloat settled particles. Such a simplification derives from the assumption that settling plastics reach the sea bottom quickly enough to neglect the effect of the vertical component of current transport. Specific particle shape and size are not set because only the case of macroplastics with known w_s (equal or greater than zero mm/s) in the absence of biofouling and degradation processes is considered. Forward simulations are performed to obtain the particle pathways from fixed sources with an hourly time step and their final fate (i.e. final position in water, on the beach or out of the numerical domain).

2.4.3. Simulations

Existing studies reveal a marked seasonal variability in the distribution of marine plastic litter in the Mediterranean Sea, caused by the seasonal weakening of some coastal and offshore currents (Macias et al., 2019; Mansui et al., 2020). Therefore, as reported in Table 5, hydrodynamic scenarios representing the four seasons (i.e. winter from December to February, spring from March to May, summer from June to August and autumn from September to November) are defined instead of sequences of real events, considering five days runs to ensure the stabilization of the results. For each one of the four seasons, different combinations of external forcing are tested, in order to separately analyze the effects of astronomical tide, waves and wind on current velocities. In particular, the astronomical tide is defined through its harmonic components. The choice to force the open boundary of the model domain with harmonic tidal elevation and the surface boundary with a wind field is a commonly employed approach for coastal regions as in the present work (e.g. Sousa et al., 2021; Wisha et al., 2022; Cardoso and Caldeira, 2021). Compared to previous studies, we also set a wave open boundary condition to include the wave-generated longshore currents and the Stokes drift, and point river discharges. In this regard, the effects on the particle vertical displacement and mixing of the saline gravity current generated at the river mouth should be also considered, because they may be significant, as demonstrated by experimental (e.g. Robinson et al., 2013; Musumeci et al., 2017; Stancanelli et al., 2018a; Marino et al., 2023) and numerical studies (e.g. Stancanelli et al., 2018b; Viviano et al., 2018; Cui et al., 2022) on gravity currents in marine environments. However, since here the focus is on the nearshore plastic transport, the detailed modelling of the estuary processes is out of the scope of the present work.

Stationary wind and wave fields representative of each season are computed on the basis of the reanalysis datasets described in Section 2.2, and then combined with stationary river floods and periodic astronomical tide. Concerning wave conditions, for each of the fixed 11 boundary points (Fig. 4), a representative mean sea state is calculated for each season. The representative significant wave height is the one which corresponds to the averaged total mean wave energy calculated for the considered season. The total mean wave energy per surface unit (E) is calculated using the following formula:

$$E = \frac{1}{8}\rho_w H_s^2 \tag{5}$$

where ρ_w is the water density. The peak wave periods associated to the representative H_s are calculated using an empirical relationship. In particular, the formula proposed by Boccotti (2004) is adapted to the wave data of the study area:

$$T_p = 14.82\pi\sqrt{\frac{H_s}{4g}} \tag{6}$$

The direction of wave propagation for the representative sea state is

Table 5
Summary of the performed hydrodynamic simulations.

Simulation	Season	Astronomical tide	Wave conditions	Wind conditions	River discharges
Winter_01	Winter	X	Mean	Mean	–
Winter_02		X	Mean	–	–
Winter_03		–	Mean	–	–
Winter_04		X	–	–	–
Winter_05		X	Mean	Mean	$T_r = 2$ years
Winter_06		X	Mean	Mean	$T_r = 50$ years
Winter_07		X	Mean	Mean	$T_r = 100$ years
Winter_08		X	$T_r = 100$ years	$T_r = 100$ years	$T_r = 100$ years
Summer_01	Summer	X	Mean	Mean	–
Summer_02		X	Mean	–	–
Summer_03		–	Mean	–	–
Summer_04		X	–	–	–
Spring_01	Spring	X	Mean	Mean	–
Spring_02		X	Mean	–	–
Spring_03		–	Mean	–	–
Spring_04		X	–	–	–
Autumn_01	Autumn	X	Mean	Mean	–
Autumn_02		X	Mean	–	–
Autumn_03		–	Mean	–	–
Autumn_04		X	–	–	–

set equal to the one corresponding to the highest percentage of events.

Concerning wind conditions, the preliminary comparison between the wind velocity time-series at the three ERA5 grid points indicated in Fig. 1b showed that the study area is characterized by a uniform mean wind climate. Therefore, magnitude and direction of a constant wave field are calculated for the four seasons, considering the mean wind velocity and the direction corresponding to the highest percentage of events relative to the closest grid point to the MPA.

In addition to the representative seasonal sea state, the 100-year return period wave condition, which is more likely to occur in winter, is considered. The 100-year return period significant wave height for the 11 boundary points (Fig. 4) is derived from the extreme value analysis of the available wave data, which is performed by applying the peak over threshold (POT) method for the identification of sea storms, with a threshold equal to 2.00 m and a minimum time interval between independent events equal to 12 h (Boccotti, 2004). The peak wave periods corresponding to the 100-year return period significant wave heights are calculated using Eq. 6. The wave direction is assumed equal to the one with the highest frequency of occurrence of sea storms at the site. Similarly, the 100-year return period wind conditions are calculated on the basis of the extreme value analysis of wind data time-series. The ranges of the wave boundary conditions and the velocity and direction of the uniform wind (U_w and D_w, respectively) are shown in Table 6.

As reported in Table 5, the peak flow rates of Mazzarà, Termini and Mela rivers corresponding to return periods of 2 years (i.e. with a high frequency of occurrence), 50 years and 100 years (i.e. with a low frequency of occurrence, Table 2) are included in four of the simulations performed for the winter season. The combination of astronomical tide, representative winter mean wave and wind conditions and river discharges with different occurrence frequency is also simulated (i.e. simulations Winter_05, Winter_06 and Winter_07). Moreover, since a direct correlation between extreme marine events and rainfall is expected (Zheng et al., 2013; Xu et al., 2014; Camus et al., 2022) simulation Winter_08 is performed considering a worst-case scenario, where the 100-year return period river floods, significant wave height and wind velocity occur simultaneously.

Five plastic release points are considered (Fig. 4): i) $R1$ (latitude: 38.1502°N; longitude: 15.0551°E; water depth: 8.00 m) and $R2$ (latitude: 38.2597°N; longitude: 15.2253°E; water depth: 60.00 m) simulate the marine plastic litter coming from the sea; ii) $R3$ (latitude: 38.1392°N; longitude: 15.1327°E; water depth: 4.90 m), $R4$ (latitude: 38.1519°N; longitude: 15.1676°E; water depth: 16.70 m) and $R5$ (latitude: 38.1838°N; longitude: 15.2064°E; water depth: 30.00 m) correspond to the mouths of Mazzarà, Termini and Mela rivers, respectively. Even if the river discharges are null, we assume that beached plastics close to the mouth reach the sea under the action of wind and waves. Four-days long preliminary simulations are performed by releasing 10 particles at each seeding site for a total of 50 particles, which is a sufficient number to ensure the significance of sensitivity analyses (Jalón-Rojas et al., 2019) as well as acceptable computational times (i.e. about one hour using a processor Intel Core i7–9700 3.00 GHz). Additionally, further simulations are performed by releasing 1000 particles at each source for a total of 5,000 particles (computational time of about 80 h) to identify marine plastic accumulation zones.

Table 7 summarizes the input data of the performed particle tracking simulations. The four hydrodynamic scenarios corresponding to winter, summer, spring and autumn in the presence of astronomical tide, waves and wind (i.e. Winter_01, Summer_01, Spring_01 and Autumn_01) and the ones which include the 2-year and 100-year return period discharge of the Mazzarà, Termini and Mela rivers (i.e. Winter_05, Winter_07 and Winter_08) are employed as input data for the particle tracking simulations. A total of 84 particle tracking simulations with 50 particles are performed, i.e. 12 scenarios for each hydrodynamic condition. Moreover, 14 particle tracking simulations with 5,000 particles are run considering scenarios 3 and 10 of Table 7. Two particle behaviors are considered, i.e. macro-plastics with density higher or lower than the water density, which are both representative of the plastic samples collected in the study area (Fig. 3c). The difference between the two behaviors is that macro-plastics having ρ greater than ρ_w can settle and reach the sea bottom. The tested settling rates (w_s) ranges between 5 mm/s and 50 mm/s, in accordance with Chubarenko et al. (2016) and Kowalski et al. (2016). It is worth to point out that the effect of the inertial Stokes drift on the settling velocity is weaker for larger particles (De Leo et al., 2021; DiBenedetto et al., 2022), and hence is negligible for the macro-plastics considered in the present study. Different values of K_h were assumed, following the indications of Jalón-Rojas et al. (2019). All the simulations include the beaching process, whereas different particle refloating conditions are tested, i.e. no washing-off and washing-off with T_w equal to 1 and 2 days. Degradation and biofouling processes were not modeled, because the time scale of the simulations is not sufficiently long for the development of such processes. Finally, the hydrodynamic simulations are performed considering a uniform and constant wind field, thus the effect of the latter on plastic transport is indirectly included.

3. Results

3.1. Coastal currents

The velocity field recorded at the end of each simulation is plotted as color map, where the color scale indicates the velocity module and the arrows its direction (e.g. Fig. 5). First of all, the effects of astronomical tide on coastal currents are investigated. The analysis of the obtained velocity fields for simulations Winter_04, Summer_04, Spring_04 and Autumn_04 reveals that the astronomical tide generates cyclic onshore and offshore currents, which are able to transport sediments or floating objects, alternatively towards and away from the coast. Therefore, the astronomical tide does not contribute to the net longshore transport. As regards the module of the current velocity produced by the astronomical tide, it is of the order of 10^{-2} m/s.

Longshore currents are mainly generated by the shore-parallel component of the radiation stresses associated with the breaking process of obliquely incoming waves. The velocity fields of simulations Winter_03, Summer_03, Spring_03 and Autumn_03 (i.e. of simulations with only representative mean wave motion) allow the quantification of the velocity of such longshore currents. For instance, Fig. 5 shows the velocity field at the end of simulation Winter_03, with a zoom on the region of the MPA. The highest current velocities develop near the shore, and they are of the order of 10^{-1} m/s, i.e. one order of magnitude higher than the ones associated with the astronomical tide. However, the

Table 6
Ranges of wave and wind boundary conditions employed for the hydrodynamic simulations (the ranges indicate the variability of the 11 points of the boundary).

Season	Condition	Waves			Wind	
		H_s [m]	T_p [s]	D_m [°N]	U_w [m/s]	D_w [°N]
Winter	Mean	0.91÷1.27	6.85÷7.88	275.5÷332.9	4.84	270.0
	$T_r = 100$ years	4.22÷7.44	15.26÷20.00	281.25÷326.25	19.03	270.0
Summer	Mean	0.67÷0.84	6.01÷6.62	280.3÷331.8	2.87	293.0
Spring	Mean	0.82÷1.10	6.53÷7.37	261.5÷333.3	4.09	276.0
Autumn	Mean	0.79÷1.09	6.45÷7.34	279.8÷341.5	3.72	274.0

Table 7
Summary of the performed particle tracking simulations.

Hydrodynamic simulation	Behavior	No. of particles	Scenario	K_h [m^2/s]	Beaching	T_w [days]	w_s [mm/s]
Winter_01, Winter_05, Winter_07, Winter_08, Summer_01, Spring_01, Autumn_01	$\rho \leq \rho_w$	50	1	1	yes	–	–
		50	2	1	yes	1	–
		50 and 5,000	3	5	yes	1	–
		50	4	10	yes	1	–
		50	5	1	yes	2	–
		50	6	1	yes	–	5
		50	7	1	yes	1	5
		50	8	1	yes	1	10
	$\rho > \rho_w$	50	9	1	yes	1	50
		50 and 5,000	10	5	yes	1	5
		50	11	10	yes	1	5
		50	12	1	yes	2	5

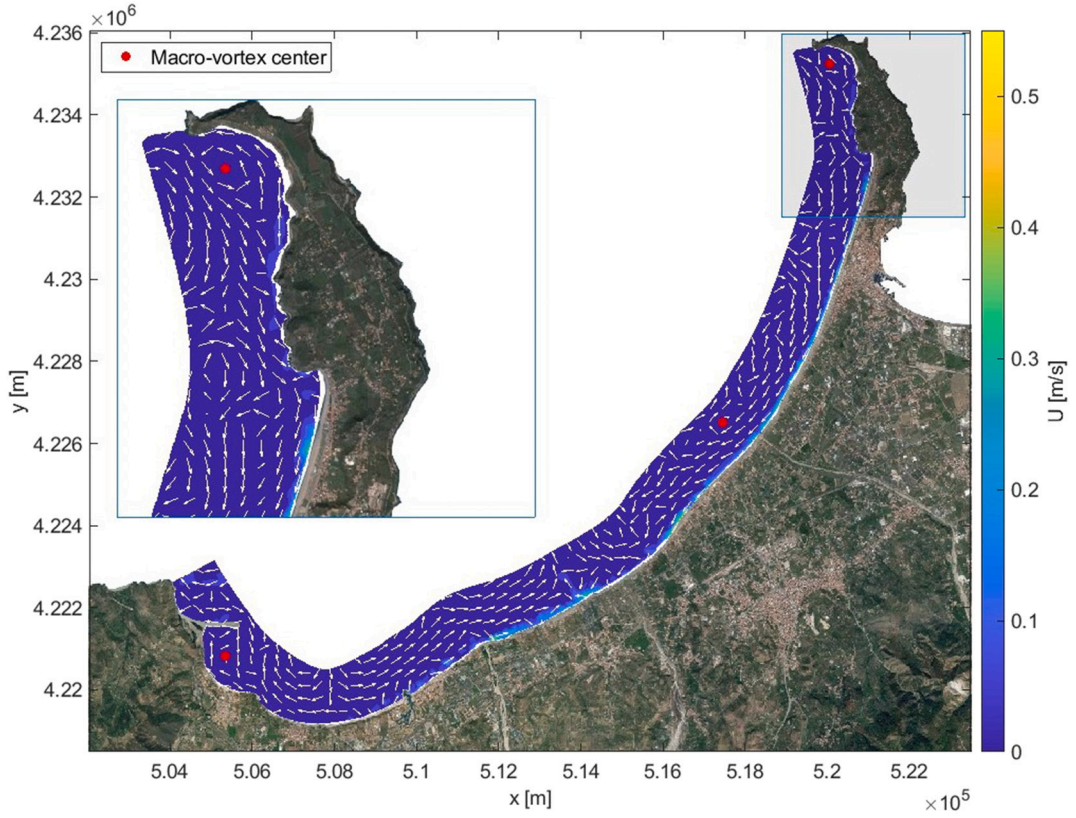

Fig. 5. Velocity field at the end of simulation Winter_03, with zoom on the region of the MPA of Capo Milazzo.

direction of the longshore currents over the whole domain is not unique. Indeed, several macro-vortexes are generated, due to the bottom morphology. Since these are potential debris accumulation zone, their localization is fundamental for the strategic planning of interventions for the removal of marine plastic litter. In Fig. 5, the macro-vortexes identified for simulation Winter_03 are highlighted. In particular, the circulation cell in the region of Capo Milazzo is likely to significantly influence the plastic litter transport near the MPA. Such a macro-vortex and the one detected immediately South of Tindari are observed also during summer, spring and autumn conditions. The analysis of the results of the simulations with both astronomical tide and representative mean wave motion (i.e. simulations Winter_02, Summer_02, Spring_02 and Autumn_02) confirms that the influence of astronomical tide on longshore currents velocity module is negligible compared to the action of wave motion. However, the astronomical tide may induce a different spatial distribution of the macro-vortexes. In any case, the macro-vortex generated in the vicinity of the MPA is present also when the contribution of the astronomical tide is considered.

Wind blowing towards a certain direction is expected to enhance the coastal current velocity along such a direction. In order to quantify the contribution of wind on coastal currents for each season, maps of the differences between the velocity fields generated by astronomical tide, waves and wind (i.e. of simulations Winter_01, Summer_01, Spring_01 and Autumn_01) and by only astronomical tide and representative mean wave motion (i.e. of simulations Winter_02, Summer_02, Spring_02 and Autumn_02) are reported in Fig. 6. A general positive variation of the velocity module (ΔU_{wind}) is observed, with a maximum of +0.11, + 0.05, +0.08 and +0.06 m/s for winter, summer, spring and autumn, respectively. Such a result is due to the fact that the wave-generated longshore currents have a prevalent component along the same direction of the wind. A reduction of the velocity module due to wind occurs only in the correspondence of limited recirculation zones characterized by velocities opposite to the wind direction.

The effects of river floods on the velocity fields are also analyzed, using the outputs of simulations Winter_05, Winter_06 and Winter_07 (i.e. simulations for the winter season with astronomical tide, represen-

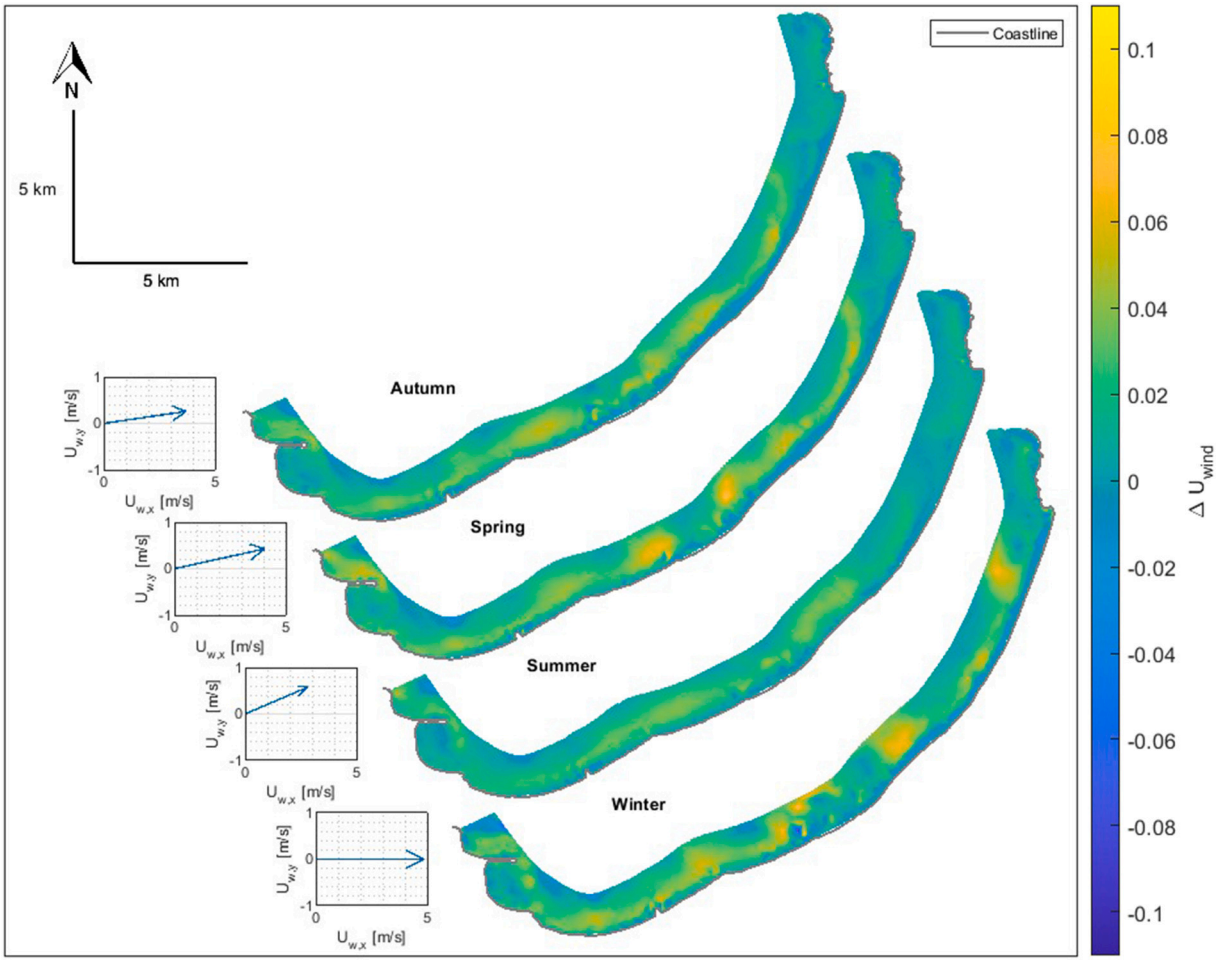

Fig. 6. Difference between the velocity fields at the end of simulations with and without wind field for the four seasons. The horizontal and vertical components of the wind velocity included in simulation Winter_01, Summer_01, Spring_01 and Autumn_01 ($U_{w,x}$ and $U_{w,y}$, respectively) are also plotted.

tative mean wave conditions, wind and river discharges corresponding to T_r equal to 2, 50 and 100 years, respectively). For the sake of simplicity, Fig. 7 shows only the velocity field of simulation Winter_07, with reference to the coastal areas near the mouths of the rivers Mazzarà, Termini and Mela. The color maps reveal a general increase of the longshore current velocity close to the river mouths with respect to simulation Winter_01, up to 1.89, 2.52 and 2.78 m/s for return periods equal to 2, 50 and 100 years, respectively. Such maximum velocities are reached in the region of the river Termini, confirming the significant role of river floods in the transport of plastic litter. Indeed, rivers not only drive the plastic waste produced inland by agricultural, industrial and urban activities into the sea, but also enhance its longshore spreading, above all during the most extreme flow events. The longshore and cross-shore widths (i.e. W_{long} and W_{cross}) of the regions where velocity is larger than the results of simulation Winter_01 (equal to or greater than 0.10 m/s) are measured in order to give a measure of the extension of the area of influence of each river (Table 8). The areas influenced by the river floods expand along the longshore direction almost symmetrically, reaching width up to about 7 km for the 100-year return period event of the Mazzarà river. Along the offshore direction, the width of the areas influenced by the river floods is limited, with values of the order of hundreds of meters.

Similarly to simulation Winter_07, simulation Winter_08 includes the effects of astronomical tide, wind, wave and 100-year return period river floods. Wind and wave conditions are representative of less frequent but more intense events, having the same return period of the river floods. As a consequence, the velocity field of simulation Winter_08 presents higher current velocities than the ones of simulation Winter_07, about 7 % larger on average. Concerning the current directions, for simulation Winter_08 a clear longshore orientation is observed not only close to the coast like in simulation Winter_07, but over the whole numerical domain.

3.2. Sensitivity analysis of the particle tracking model

The relative influence of different processes on macro-plastic trajectories and fates is assessed by combining qualitative and quantitative analyses. Since similar results are found for all the tested hydrodynamic conditions, in the following only the outputs of the particle tracking simulations performed with 50 particles under hydrodynamic condition Winter_01 are compared and discussed. Moreover, for the sake of simplicity only the most significant results relative to scenarios 2, 4, 5, 7, 9, 11, and 12 are discussed, using as benchmark scenarios 1 and 6 (Table 7) for the case of buoyant and non-buoyant particles, respectively.

Fig. 8 shows the particle trajectories and fates for the above-mentioned scenarios under hydrodynamic condition Winter_01. The comparison between buoyant and non-buoyant particles for the same values of K_h and T_w, i.e. between scenarios 2, 4 and 5 (Fig. 8a) and 7, 11 and 12 (Fig. 8b), reveals that the sedimentation process significantly influences the transport of plastic litter, to a greater extent for particles released by R1, R3 and R4 sources, which are located at the lower water depths. Such a result is due to the fact that particles settle faster in lower water depths, thus accumulating at the bottom near the release point

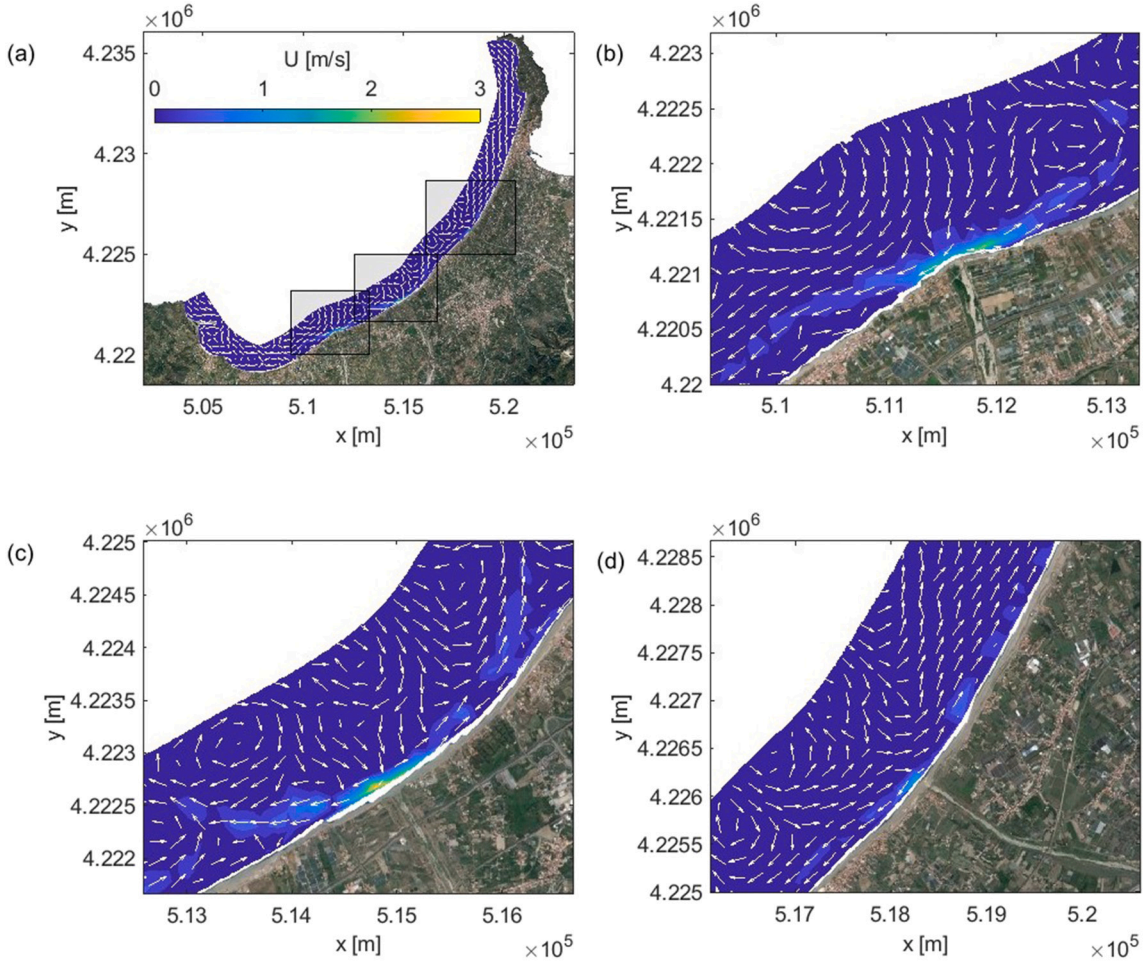

Fig. 7. Velocity field at the end of simulation Winter_07 for the regions highlighted in panel (a): (b) Mazzarà river; (c) Termini river; (d) Mela river.

Table 8
Longshore and cross-shore widths of the regions where velocity increments due to the peak flow rates are equal to or greater than 0.10 m/s, in the presence of winter representative mean wave and wind conditions.

River	Width [m]	$T_r = 2$ years (Winter_05)	$T_r = 50$ years (Winter_06)	$T_r = 100$ years (Winter_07)
Mazzarà	W_{long}	4544.70	5081.78	6951.47
	W_{cross}	304.57	309.16	347.72
Termini	W_{long}	3116.33	4631.93	4261.24
	W_{cross}	142.43	151.43	201.07
Mela	W_{long}	4661.45	6060.71	4845.03
	W_{cross}	118.65	142.03	480.22

and stopping earlier their spreading into the sea. The comparison between scenarios 7 and 9 highlights that, for macro-plastics with $\rho > \rho_w$, higher values of w_s significantly reduce the particle traveled distance from the release point and enhances the number of settled particles (Fig. 8b).

The effects of horizontal dispersion and washing-off processes on the particle tracking results are also investigated. For increasing K_h, trajectories followed by particles with $\rho \leq \rho_w$ are characterized by narrower spreading areas and by a less linear progression (scenarios 2 and 4 in Fig. 8a). As a consequence of the increased turbulent dispersion, the number of particles that move near the coastline and reach the land is higher. Moreover, for higher K_h the refloated particles are more likely to move away from the coastline. The same results are found for particles with $\rho > \rho_w$, by comparing trajectories and fates of scenarios 7 and 11 (Fig. 8b). It should be noted that the transport of particles that immediately settle in the vicinity of their source is not affected by changes in the horizontal modelling of the dispersion process.

As regards the washing-off process, small changes in trajectories and destinations are found for both buoyant (scenarios 2 and 5 in Fig. 8a) and non-buoyant particles (scenarios 7 and 12 in Fig. 8b) for different values of T_w. In particular, despite of the value of T_w, no difference are observed for the trajectories and fates corresponding to the release point R2 (i.e. in the vicinity of the MPA). For the other plastic sources, buoyant refloated particles, which in some cases suffer repeated beaching and washing-off processes, travel short distances, thus remaining close to the first beaching area.

The above qualitative results are confirmed by the quantitative comparison between the particle trajectories as well as by the calculation of the number of macro-plastics for each possible fate. The first analysis is based on the calculation of the skill score, which is a measure of the differences between two trajectories. If the two trajectories are identical, it is equal to 1, otherwise it assumes positive values as smaller as the discrepancies increase. In particular, it is defined as follows (Liu and Weisberg, 2011):

$$ss = \begin{cases} 1 - c/n & (c \leq n) \\ 0 & (c > n) \end{cases} \tag{7}$$

where n is a tolerance threshold here assumed equal to 1 (Liu and Weisberg, 2011; Jalón-Rojas et al., 2019), and c is the normalized cumulative Lagrangian separation distance between the reference and analyzed trajectories (i.e. the ratio between the cumulative Lagrangian separation distance and the cumulative length of the reference trajectory). The skill score has been widely employed for the comparison

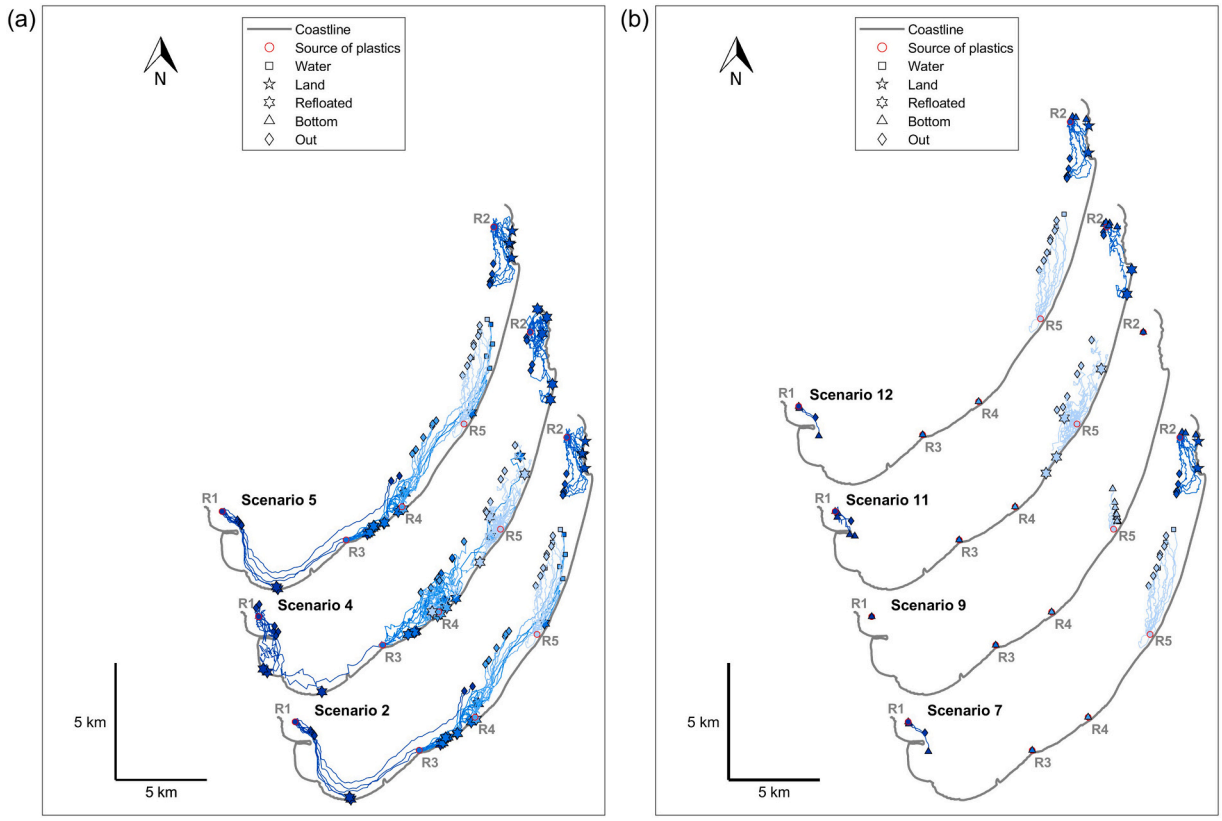

Fig. 8. Sources, trajectories and fates of 50 macro-plastics under hydrodynamic condition Winter_01: (a) buoyant particles (scenario 2: $K_h = 1$ m^2/s, beaching/washing-off on, $T_w = 1$ day; scenario 4: $K_h = 10$ m^2/s, beaching/washing-off on, $T_w = 1$ day; scenario 5: $K_h = 1$ m^2/s, beaching/washing-off on, $T_w = 2$ day); (b) non-buoyant particles (scenario 7: $K_h = 1$ m^2/s, beaching/washing-off on, $T_w = 1$ day, $w_s = 5$ mm/s; scenario 9: $K_h = 1$ m^2/s, beaching/washing-off on, $T_w = 1$ day, $w_s = 50$ mm/s; scenario 11: $K_h = 10$ m^2/s, beaching/washing-off on, $T_w = 1$ day, $w_s = 5$ mm/s; scenario 12: $K_h = 1$ m^2/s, beaching/washing-off on, $T_w = 2$ days, $w_s = 5$ mm/s). Different color shades are employed to distinguish trajectories originated from different plastic sources.

between observed and modeled trajectories of oil spills at sea (Liu and Weisberg, 2011; Röhrs et al., 2012; Liu et al., 2014; Sayol et al., 2014). Moreover, such an index has been recently used to perform the sensitivity analysis of particle tracking models (Jalón-Rojas et al., 2019).

In the present work, the skill score of the trajectory of each released particle with respect to a reference scenario is calculated, and then the corresponding mean value (ss_m) for each plastic source is estimated. Scenarios 1 and 6 of Table 7 are selected as reference scenarios for the assessment of the influence of the horizontal dispersion and washing-off processes on the particles trajectories and fates, to distinguish between buoyant and non-buoyant particles. Moreover, scenario 6 is the benchmark for the investigation of the effects of w_s variations on the particle tracking results. Fig. 9a-b shows the mean skill score (ss_m) for scenarios 2, 4, 5, 7, 9, 11 and 12 under hydrodynamic condition Winter_01, which is calculated as the average of the ten skill scores obtained for each plastic source. The mean skill score calculated for scenarios 2 and 5 (Fig. 9a) and scenarios 7 and 12 (Fig. 9b) is equal to 1 for all the macro-plastic sources with the exception of R3 releasing buoyant particles, for which ss_m is about 0.50 for scenarios 2 and 5. In such a case, macro-plastics that under scenario 1 beached in the vicinity of the release point travel distances not longer than 2 km, moving parallel to the shore towards the MPA. Therefore, the washing-off process is confirmed to influence only slightly particle tracking results. Fig. 9a-b also shows that ss_m calculated for scenarios 4 and 11 assumes values ranging between 0.29 and 0.69, which are different from the ones corresponding to scenarios 2 and 7, respectively. The only exceptions are observed for sources R3 and R4, for which all the particles settle as soon as released, despite of the employed K_h. Such a result confirms that the horizontal dispersion process significantly influences the plastic transport, above all when the particle settling is not included. The lowest values of ss_m are found for the case of buoyant particles released at the river mouths (i.e. R3, R4 and R5 release points). Concerning the sedimentation process, Fig. 9b shows that ss_m ranges between 0.55 and 1.00 for scenarios 8 and 9, which are characterized by higher w_s than scenarios 6 and 7. It should be noted that ss_m is equal to 1 when the particles settle as soon as released regardless of the assumed w_s.

The outcomes of the second quantitative analysis of the difference between the simulated scenarios are showed in Fig. 9c, which reports the percentage of particles that at the end of the simulations are in the water, on the beach, refloated from the beach, at the sea bottom or out of the numerical domain, with reference to the hydrodynamic condition Winter_01. The simulations with buoyant macro-plastics (i.e. scenarios 1, 2, 4 and 5) end with about 50 % of the particles out of the numerical domain, whereas for the ones with non-buoyant plastics (i.e. scenarios 6, 7, 9, 11 and 12) the most frequent fate is the sedimentation at the bottom, with percentages between 64 % and 100 %. Despite of the employed T_w, the washing-off process causes the release of some buoyant beached particles, thus implying the reduction of the percentage of beached macro-plastics from 34 % of scenario 1 to 8 % of scenario 5. The total number of floating particles, both refloated or not, increases accordingly. Instead, when non-buoyant particles are considered (i.e. scenarios 6 and 12) the washing-off process does not affect the final destination of the particles, which are almost all at the bottom or out of the domain. The enhancement of the horizontal dispersion process produces the increase of the percentage of refloated buoyant particles, from the minimum 26 % of scenario 2 to the maximum 44 % of scenario 4. For the cases of non-buoyant particles (i.e. scenarios 7 and 11), the influence of K_h on particle fates is less evident, because of the most

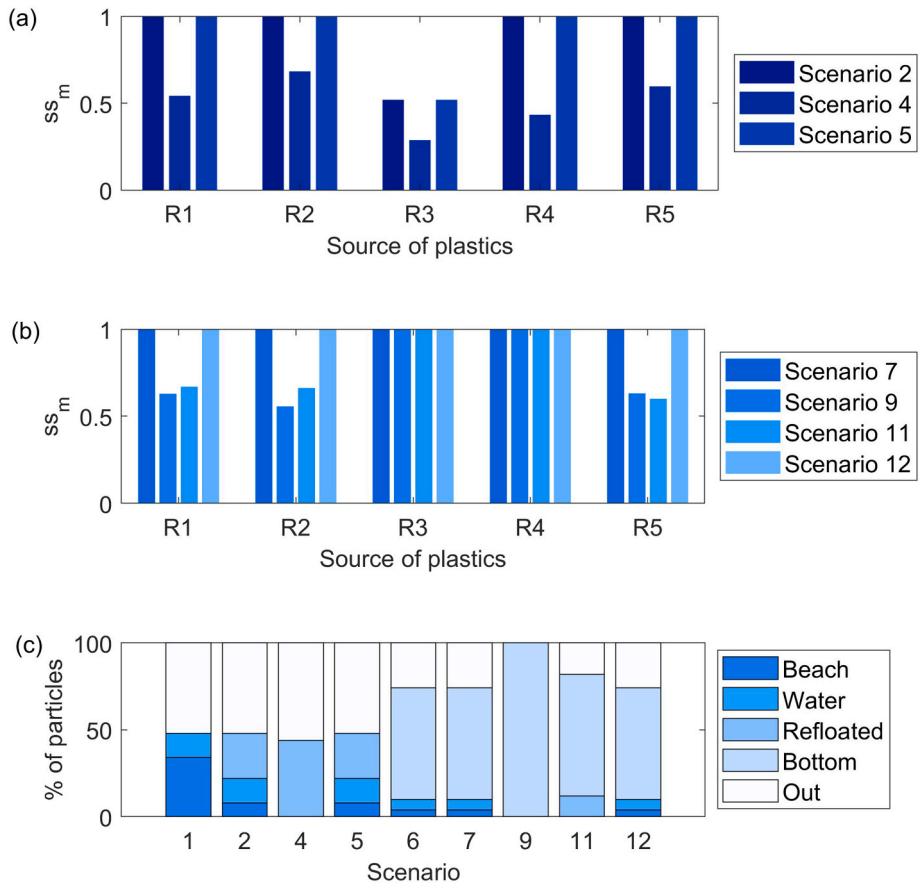

Fig. 9. Comparison between 50 macro-plastic trajectories and fates under hydrodynamic condition Winter_01: (a) mean skill scores of the trajectories followed by buoyant particles released by R1, R2, R3, R4 and R5 sources, having scenario 1 as reference ($K_h = 1$ m^2/s, beaching/washing-off on); (b) mean skill scores of the trajectories followed by non-buoyant particles released by R1, R2, R3, R4 and R5 sources, having scenario 6 as reference ($K_h = 1$ m^2/s, beaching/washing-off on, $w_s = 5$ mm/s); (c) fates of the particles (scenario 2: $K_h = 1$ m^2/s, beaching/washing-off on, $T_w = 1$ day; scenario 4: $K_h = 10$ m^2/s, beaching/washing-off on, $T_w = 1$ day; scenario 5: $K_h = 1$ m^2/s, beaching/washing-off on, $T_w = 2$ day; scenario 7: $K_h = 1$ m^2/s, beaching/washing-off on, $T_w = 1$ day, $w_s = 5$ mm/s; scenario 9: $K_h = 1$ m^2/s, beaching/washing-off on, $T_w = 1$ day, $w_s = 50$ mm/s; scenario 11: $K_h = 10$ m^2/s, beaching/washing-off on, $T_w = 1$ day, $w_s = 5$ mm/s; scenario 12: $K_h = 1$ m^2/s, beaching/washing-off on, $T_w = 2$ days, $w_s = 5$ mm/s).

relevant role of the sedimentation process.

3.3. Trajectories and fates of macro-plastics

3.3.1. Effects of seasonality on plastic transport

Seasonality of coastal currents is assessed through the comparison of the velocity fields in the presence of astronomical tide, waves and wind obtained for summer, spring and autumn (i.e. simulations Summer_01, Spring_01 and Autumn_01) with the one calculated for winter (i.e. simulation Winter_01). In particular, for each grid point of the numerical domain, the winter current velocity module is subtracted to the summer, spring and autumn one, thus obtaining maps showing the difference ΔU_{winter} (Fig. 10a). The obtained maps reveal that within about 95 % of the domain the absolute value of ΔU_{winter} is lower than 0.05 m/s, thus demonstrating that the differences between winter and summer, spring and autumn are modest when mean wave and wind conditions are considered. However, significant decrease of the current velocity module with respect to the winter season are observed near the coastline, to a greater extent for summer. In particular, reductions of the current velocity up to about −0.40 m/s are detected. Such a result is in agreement with the fact that winter and summer are characterized by the most and the less energetic wind and wave climate, respectively. Only some small regions are characterized by summer, spring and autumn current velocities slightly higher than the winter one. Such a phenomenon is probably due to peculiarities of the bathymetry, which influences the wave transformation processes. It should be noted that, on the basis of the results discussed in Section 3.1, the astronomical tide contribution to the current velocity seasonality is negligible.

The maps showing the difference $\Delta\theta_{winter}$ between the velocity directions corresponding to summer, spring and autumn and the ones obtained for the winter season are also calculated over the whole domain (Fig. 10b). Over about 80 % of the domain, a general tendency to clockwise (i.e. positive) or counter-clockwise (i.e. negative) not greater than 60° is observed for all the three seasons. In the rest of the domain, both clockwise and counter-clockwise $\Delta\theta_{winter}$ are found, up to about ±180°. The greatest deviation of the current direction with respect to the winter season occurs in summer. Since $\Delta\theta_{winter}$ never overcomes ±180°, a complete reversal of the direction of coastal currents with respect to winter does not occur.

The effects of current seasonality on pathways and fates of macro-plastics are here discussed with reference to hydrodynamic conditions Winter_01, Summer_01, Spring_01 and Autumn_01. For the sake of simplicity, only trajectories and fates calculated for buoyant particles with K_h equal to 5 m^3/s and T_w equal to 1 day and non-buoyant particles with K_h equal to 5 m^3/s, T_w equal to 1 day and w_s equal to 5 mm/s (i.e. considering scenarios 3 and 10, respectively) are compared. Indeed, the same conclusions can be drawn from the analysis of the outputs of each scenario of Table 7. Fig. 11 shows sources, trajectories and fates of 50 macro-plastics, distinguishing their origin through different color shades and their fate through different marker shapes. For the case of buoyant

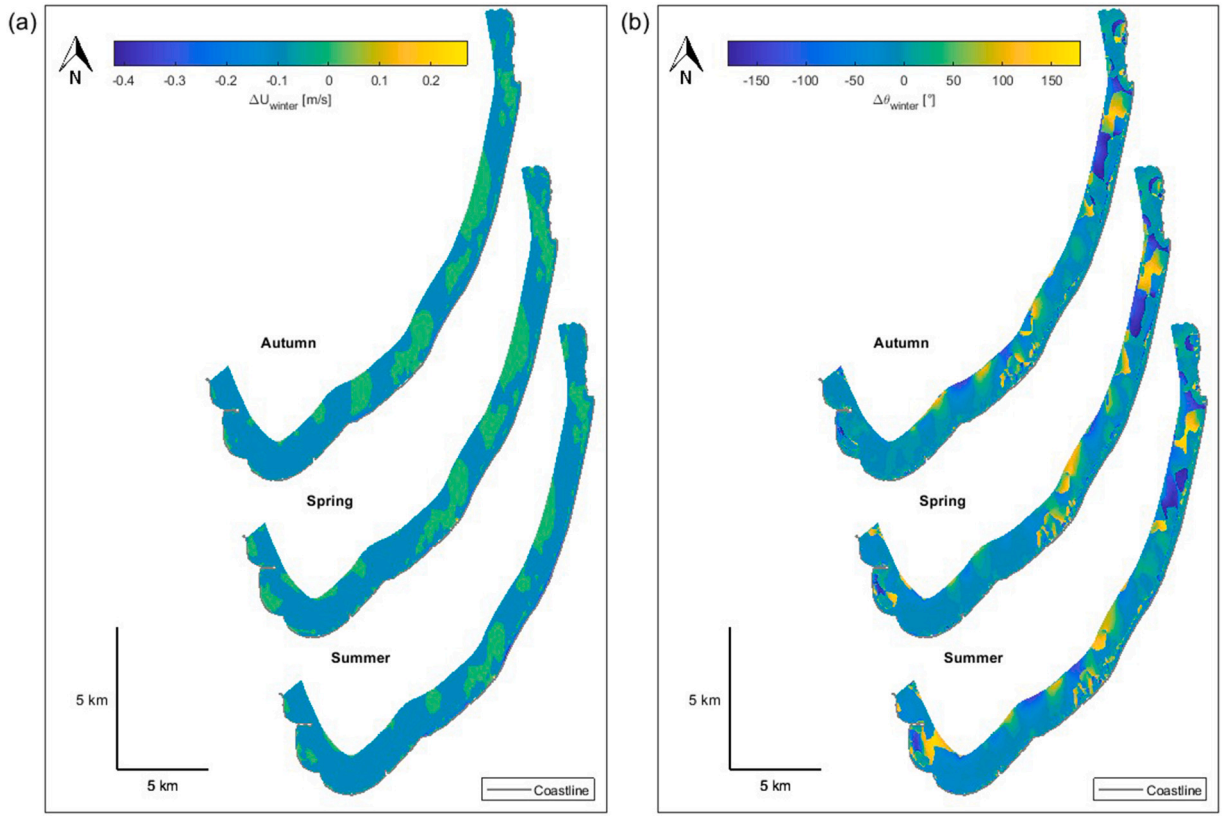

Fig. 10. Comparison between the velocity fields at the end of simulations Summer_01 (summer), Spring_01 (spring) and Autumn_01 (autumn) and the one at the end of simulation Winter_01 (winter): (a) difference between the velocity modules; (b) difference between the velocity directions.

particles (Fig. 11a), the released plastics move following similar patterns under all the four hydrodynamic conditions. Particles coming from the release point R1 tend always to reach the beach South of Tindari. Macro-plastics released by source R2 are transported towards the South without leaving the region of the MPA. The relatively short route of such particles is likely due to the macro-vortex originated close to the MPA. Finally, macro-plastics coming from the release points R3, R4 and R5 move towards the MPA under all the considered hydrodynamic conditions. Seasonality influences only the length of the pathways of such particles, which gradually decreases for winter, spring, autumn and summer. In particular, the winter pathways can be about two times longer than the summer ones. The observed trajectories are consistent with the results on the current seasonality represented in Fig. 10. Indeed, the area close to the sources R3, R4 and R5 are characterized by higher ΔU_{winter} with respect to the regions of release points R1 and R2. Moreover, the detected variations in current direction are so limited they do not cause relevant changes in plastic pathways.

The above-discussed findings are valid also for the case of non-buoyant particles (Fig. 11b), even if the tendency of plastics to reach the sea bottom softens their implications. Despite the considered season, particles released by source R1 settle close to it, whereas the ones originated from source R2 move towards the South, ending their path on the beach or at the sea bottom. Particles released by sources R3 and R4 sink close to the origin points. Finally, plastics coming from the release point R5 are always transported towards the MPA, following routes of decreasing length for winter, spring, autumn and summer respectively.

Fig. 12 shows sources, final spatial distribution and fates of 5,000 macro-plastics under each of the four seasons. In the case of buoyant particles (Fig. 12a), beached macro-plastics cover almost the whole coastline under each hydrodynamic condition. However, it is possible to identify stretches of the coast where a greater concentration of beached particles is observed. The results indicate that, the MPA of Capo Milazzo is a macro-plastic hot-spot, independently from the considered season. The same holds for Torretta beach and the Northern part of Caldera beach, which are located immediately North and South of the mouth of the Mela river, respectively. Also Marchesana beach is a macro-plastic accumulation zone under each season, particularly the Southern part near to the mouth of the Mazzarà river. Finally, the beach between the mouth of the Mazzarà river and Oliveri is another hot-spot for beached particles, despite of the considered season. In summer and autumn, also the beach between Oliveri and Tindari captures a huge number of macro-plastics. The distribution of floating particles, both refloated or not, appears to be significantly influenced by seasonality. Indeed, during winter floating macro-plastics are concentrated North of the mouth of the Mela river and near the mouth of the Termini river. Instead, during summer and spring, also the area between the mouths of the Mela and Termini river is covered by floating particles. Finally, in autumn floating particles accumulate North of the mouth of the Mela river or exit the domain.

In the case of non-buoyant particles (Fig. 12b), beached plastics are concentrated in the MPA of Capo Milazzo and in Torretta beach under each hydrodynamic condition. In winter and spring and autumn, the Northern part of Caldera beach is also a macro-plastic hot-spot. Floating particles are always concentrated North of the mouth of the Mela river. Finally, as already observed in Fig. 11b, at the smallest water depths particles immediately settle near their origin. This is the case of the seeding points R1, R2, and above all R3 and R4.

Fig. 13 summarizes the results regarding the macro-plastic fate at the end of simulations performed for the four seasons with 5,000 released particles. For the case of buoyant macro-plastics, the percentages of particles that end their pathway in water, beached or out of the numerical domain suffer slight modifications due to seasonality, with the exception of autumn. In particular, for the case of buoyant particles (Fig. 13a), the percentage of beached macro-plastic suffers contained

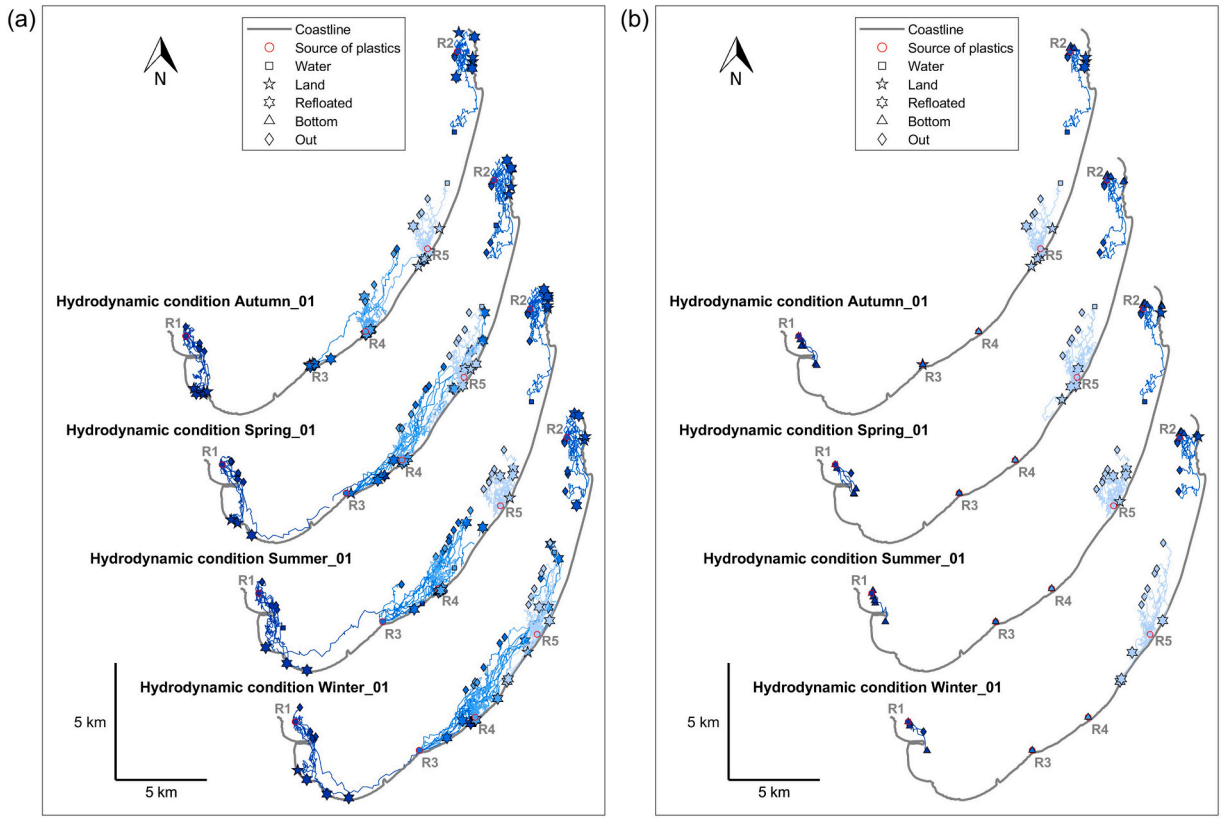

Fig. 11. Sources, trajectories and fates of 50 macro-plastics under four hydrodynamic conditions representing winter (Winter_01), summer (Summer_01), spring (Spring_01) and autumn (Autumn_01) with representative mean wave and wind conditions: (a) buoyant particles, scenario 3 ($K_h = 5\ \mathrm{m^2/s}$, beaching/washing-off on, $T_w = 1$ day); (b) non-buoyant particles, scenario 10 ($K_h = 5\ \mathrm{m^2/s}$, beaching/washing-off on, $T_w = 1$ day, $w_s = 5$ mm/s). Different color shades are employed to distinguish trajectories originated from different plastic sources.

increments in winter, summer and spring, ranging between 7 % and 14 %. On the contrary, the percentage of beached macro-plastics corresponding to autumn is significantly higher than the values calculated for the other three seasons, i.e. equal to 32 %, at the expense of the percentage of particles out of the domain. The percentage of floating particles, both refloated or not, remains almost constant under all the season and ranges between 38 % and 44 %.

The final fate of non-buoyant particles is less affected by coastal current seasonal variability, because most of them (i.e 64÷70 %) settles to the sea bottom despite the considered hydrodynamic regime (Fig. 13b). The percentage of beached macro-plastic ranges between 2 % and 4 % in winter, summer and spring, whereas it is equal to about 16 % in autumn. The overall percentage of particles which end their path in water, both refloated or not, varies in the range 9÷11%.

3.3.2. *Effects of river floods on plastic transport*

The effects of river floods on trajectories, spatial distribution and fates of macro-plastics are investigated through the comparison between the results corresponding to the winter hydrodynamic conditions which include the peak flow rates of rivers Mazzarà, Termini and Mela, namely Winter_05, Winter_07 and Winter_08, and the one with only astronomical tide and mean representative wind and wave climate, namely Winter_01. For the sake of simplicity, in the following only the cases of buoyant particles with K_h equal to 5 $\mathrm{m^3/s}$ and T_w equal to 1 day, and non-buoyant particles with K_s equal to 5 $\mathrm{m^3/s}$, T_w equal to 1 day and w_s equal to 5 mm/s (i.e considering scenarios 3 and 10, respectively) are considered. Anyway, the same findings can be obtained from the analysis of the outputs of each scenario of Table 7.

Fig. 14 shows pathways and final destinations of 50 macro-plastics under Winter_05, Winter_07 and Winter_08 hydrodynamic conditions. For the case of mean representative wind and wave climate and 2 and 100-year return period river floods (i.e. hydrodynamic conditions Winter_05 and Winter_07, respectively), trajectories of both buoyant and non-buoyant macro-plastics released by sources R1 and R2 are quite similar to the case Winter_01 reported in Fig. 8. However, macro-plastics released by sources R1 tend to stop their routes further from the mouth of river Mazzarà with respect to the benchmark. Similarly, macro-plastics released from source R2 travel shorter distances, thus concentrating in the region of the MPA. Instead, the transport of buoyant particles coming from release points R3 and R4 totally change its direction with respect to the benchmark. When significant river floods occur, macro-plastics move not towards the MPA, but towards Tindari, with higher velocity corresponding to the 100-year return period. For the case of non-buoyant particles, no differences between the results found for Winter_05, Winter_07 and the benchmark Winter_01 are observed, because all the particles settle as soon as released. Finally, both buoyant and non-buoyant macro-plastics released by source R5 have a greater tendency to move towards the MPA and exit the numerical domain when the river discharges are included.

The final spatial distribution of 5,000 macro-plastics under the effects of river floods is shown in Fig. 15. The results relative to hydrodynamic conditions Winter_05 and Winter_07 reveal that both buoyant and non-buoyant beached macro-plastics are more concentrated compared to the benchmark Winter_01. In particular, the MPA of Capo Milazzo is always a macro-plastic hot-spot. Instead, Torretta and Caldera beaches and the beach between Tindari and Tonnarella accumulate less buoyant particles as the magnitude of the river floods increases. The other portions of the coast are free from beached plastics. The few floating particles, both refloated or not, are mainly distributed between the MPA of Capo Milazzo and the mouth of the Mela river. Finally, the

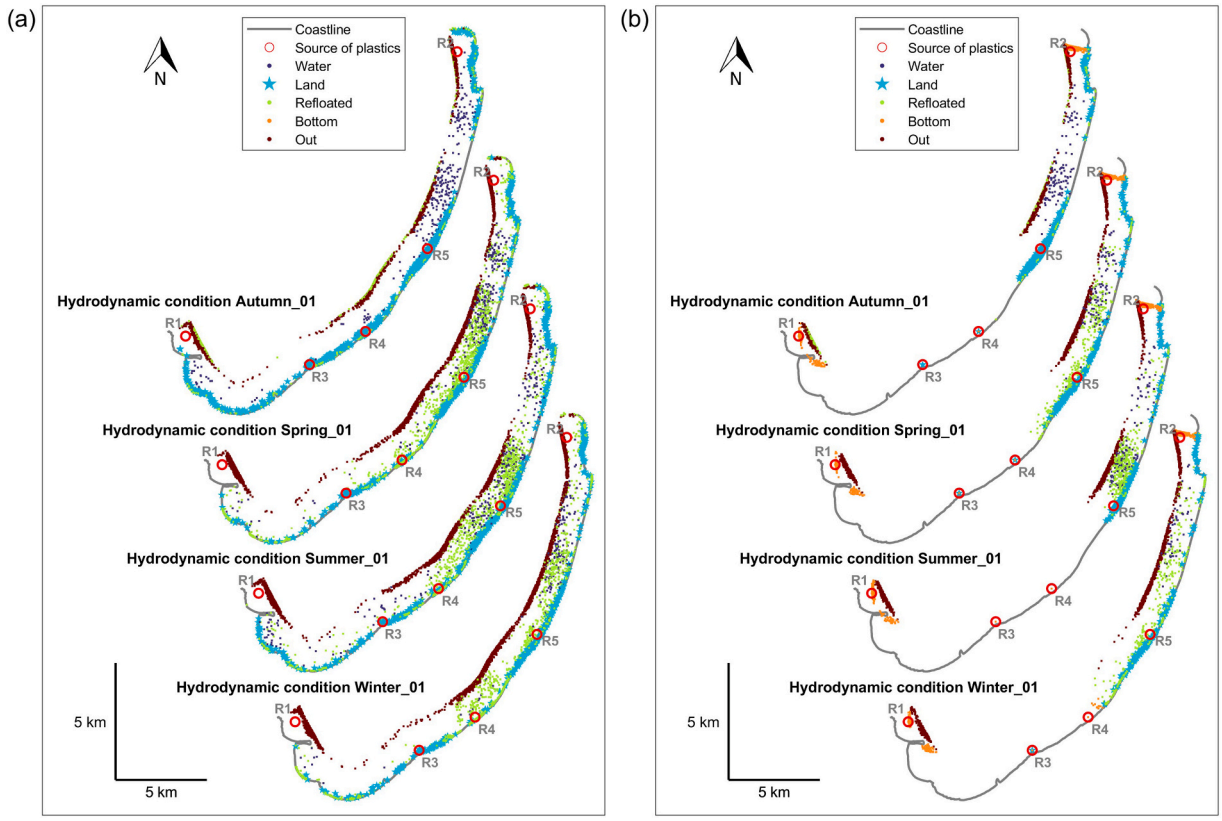

Fig. 12. Sources, final spatial distribution and fates of 5,000 macro-plastics under four hydrodynamic conditions representing winter (Winter_01), summer (Summer_01), spring (Spring_01) and autumn (Autumn_01) with representative mean wave and wind conditions: (a) buoyant particles, scenario 3 ($K_h = 5$ m^2/s, beaching/washing-off on, $T_w = 1$ day); (b) non-buoyant particles, scenario 10 ($K_h = 5$ m^2/s, beaching/washing-off on, $T_w = 1$ day, $w_s = 5$ mm/s).

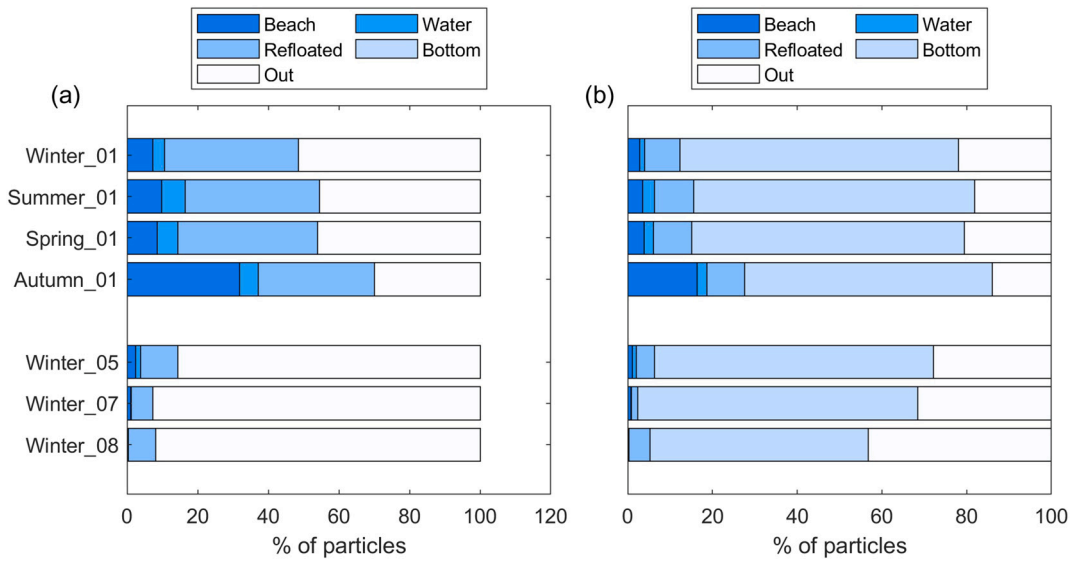

Fig. 13. Fates of 5,000 macro-plastics under seven hydrodynamic conditions representing winter (Winter_01), summer (Summer_01), spring (Spring_01) and autumn (Autumn_01) with representative mean wave and wind climate, winter with representative mean wave and wind conditions and 2-year and 100-year return period river floods (Winter_05 and Winter_07, respectively), and winter with 100-year return period wave and wind conditions and river floods (Winter_08): (a) buoyant particles, scenario 3 ($K_h = 5$ m^2/s, beaching/washing-off on, $T_w = 1$ day); (b) non-buoyant particles, scenario 10 ($K_h = 5$ m^2/s, beaching/washing-off on, $T_w = 1$ day, $w_s = 5$ mm/s).

spatial distribution of sea floor particles is not influenced by the occurrence of river floods.

Fig. 13 shows that under Winter_05 and Winter_07 hydrodynamic conditions, about 85 % of floating particles end their route out of the numerical domain. The percentage of beached macro-plastics is lower than the one calculated in the absence of river floods, being in the range 0.2÷2 % for both buoyant particles and non-buoyant particles. The percentage of settled macro-plastics is not affected by the river floods,

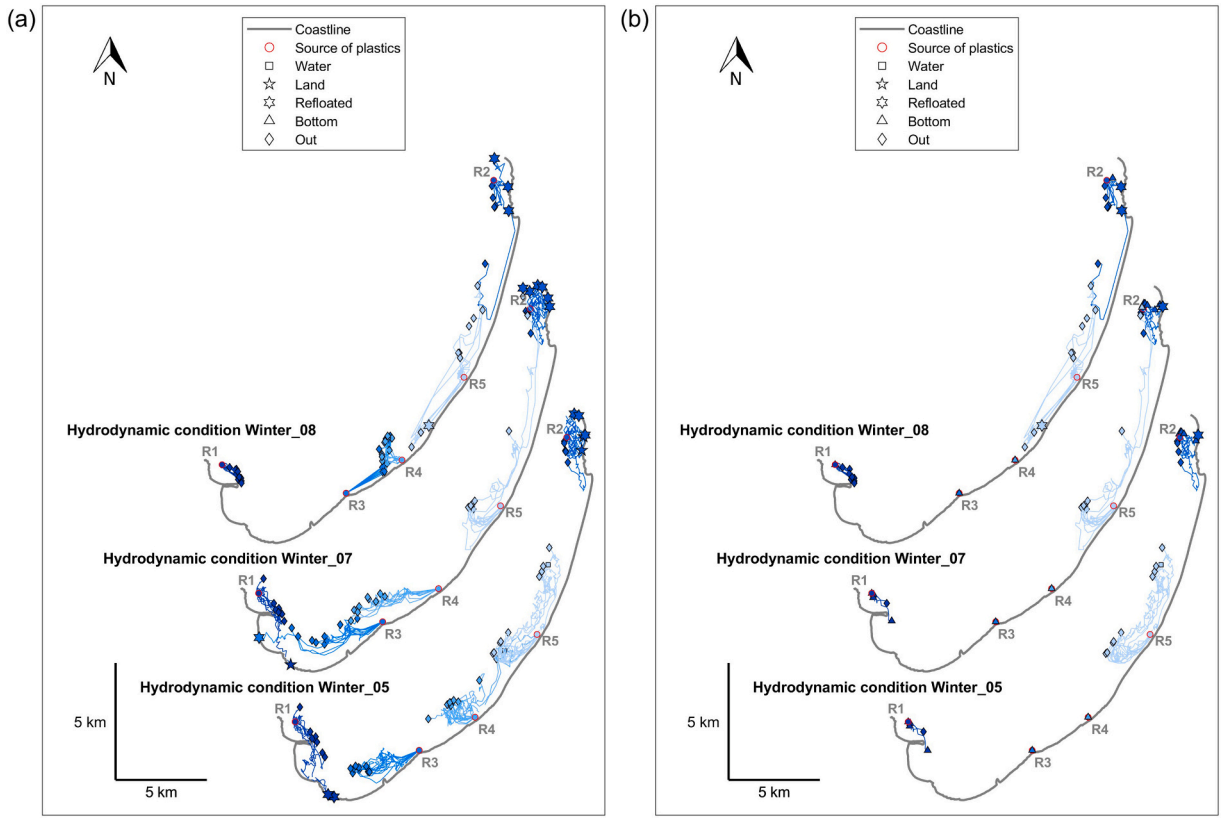

Fig. 14. Sources, trajectories and fates of plastics under three hydrodynamic conditions representing winter with representative mean wave and wind climate and 2-year (Winter_05) and 100-year (Winter_07) return period river floods, and winter with 100-year return period wind, waves and river floods (Winter_08): (a) buoyant particles, scenario 3 ($K_h = 5$ m^2/s, beaching/washing-off on, $T_w = 1$ day); (b) non-buoyant particles, scenario 10 ($K_h = 5$ m^2/s, beaching/washing-off on, $T_w = 1$ day, $w_s = 5$ mm/s). Different color shades are employed to distinguish trajectories originated from different plastic sources.

being almost constant and equal to 65 %.

Trajectories, spatial distribution and fates of macro-plastics calculated under the hydrodynamic conditions Winter_08 result from compound extreme events, namely the 100-year return period river floods, wind and wave climate. Fig. 14, Fig. 15 and Fig. 13 reveal that particles tend to exit the numerical domain, to a greater extent in the case of ρ lower than ρ_w. The beaching phenomenon is less frequent with respect to the benchmark Winter_01, and the few beached particles in the region of the MPA of Capo Milazzo and between the mouths of the Mela and Termini rivers are almost all refloated. Also the percentage of settled non-buoyant particles is lower when the combination of extreme river floods, wind and wave climate is considered, decreasing from 66 % of hydrodynamic condition Winter_01 to 52 %.

3.3.3. *Summary of the results*

The application of the proposed numerical modelling chain to the coastal area adjacent to the MPA of Capo Milazzo provides useful insights for the identification of typical directions of marine litter displacements and location of relevant beached or seafloor plastic accumulation areas in the nearshore zone, considering the effects of seasonality. The above-mentioned insights are obtained through the simulation of stationary wind and wave fields representative of each season as described in Section 2.4.3, and then combined with stationary river floods and periodic astronomical tide.

The numerical results reported in Fig. 11 show that macro-plastics released from the mouths of the Mela, Termini and Mazzarà rivers in the absence of floods which do not immediately settle are transported along the North-East direction, i.e. towards the MPA of Capo Milazzo, despite of the considered season. Also sea plastic litter released in the Western and Eastern parts of the domain follows trajectories whose direction is not influenced by the seasonality, moving towards the beach belonging to the towns of Oliveri and Falcone and to the MPA, respectively. Indeed, seasonality is only responsible of the length of the particle pathways, which gradually decreases for winter, spring, autumn and summer. As a consequence, location and extension of beached or floating macro-plastic accumulation zones are slightly different for the four seasons (Fig. 12). The effects of the Mela, Termini and Mazzarà river floods on macro-plastic transport are more evident, because they cause a total shift of the particle trajectories (Fig. 14) as well as a modification of the macro-plastic accumulation zones (Fig. 15). Therefore, for the studied site, seasonality of longshore currents is less crucial than the effects of river floods for planning interventions for the removal of macro-plastics.

In the absence of river floods, operations for the collection of floating macro-plastics should focus on the area between the mouth of the Termini river and Torretta beaches. As a matter of fact, the occurrence of river floods causes that macro-plastics exit the coastal region, moving offshore. Concerning the beached macro-plastics, they are distributed along almost the whole coastline despite of the considered season. However, the following four accumulation areas can be identified: i) the MPA of Capo Milazzo; ii) Caldera beach and northern part of Torretta beach; iii) Marchesana beach; iv) the beach between the mouth of the Mazzarà river and Oliveri. Moreover, in summer and autumn the beach between Oliveri and Tindari is also a macro-plastic hot-spot. It should be noted that the MPA of Capo Milazzo is the only area which receive macro-plastics even if river floods occur. Beach cleaning operations should be carried out preferably in autumn, when the largest quantities of beached macro-plastics are observed (Fig. 13). In accordance with Menicagli et al. (2022) and the observations of the performed field survey, such cleaning interventions should focus on the backshore zone,

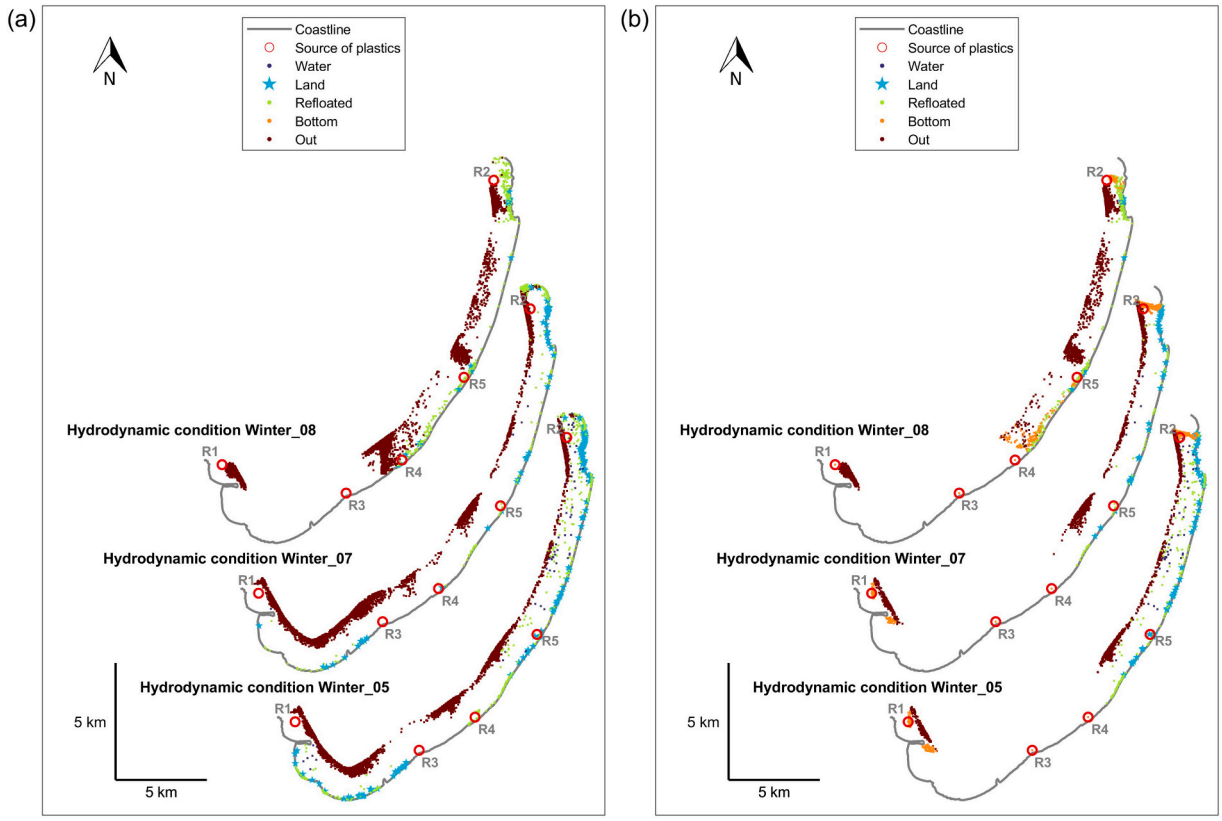

Fig. 15. Sources, final spatial distribution and fates of 5,000 plastics under three hydrodynamic conditions representing winter with representative mean wave and wind climate and 2-year (Winter_05) and 100-year (Winter_07) return period river floods, and winter with 100-year return period wind, waves and river floods (Winter_08): (a) buoyant particles, scenario 3 ($K_h = 5$ m^2/s, beaching/washing-off on, $T_w = 1$ day); (b) non-buoyant particles, scenario 10 ($K_h = 5$ m^2/s, beaching/washing-off on, $T_w = 1$ day, $w_s = 5$ mm/s).

where most of the marine litter is accumulated by intense sea storms typical of autumn and winter seasons. Finally, the position of sea floor macro-plastics appears strongly influenced by the location of the release points. Indeed, non-buoyant particles usually settle near their origins due to the relatively small depths of the study area. The only exception is represented by the particles released by the Mela river, whose mouth is located in the region with the deepest sea bottom.

Documented periodic beach clean-up campaigns in the accumulation zone derived from the numerical results (i.e. MPA of Capo Milazzo, Torretta and Caldera beaches, Marhcesana beach, and the beach of the towns of Falcone and Oliveri) demonstrate that the hydrodynamic conditions simulated in the present work are effectively representative of the study area. The presence of a relevant plastic accumulation zone in the MPA of Capo Milazzo is highlighted by the fact that beach cleaning campaigns organized by volunteer of the MPA itself or by the municipal administration were in often included in the #EUBeach-Cleanup program of the European Commission. The fact that MPA of Capo Milazzo is a litter accumulation area is also confirmed by the results of the monitoring activities carried out during the years 2020–2021 in the context of the INTERREG Med Plastic Busters MPAs project and presented at the project final conference (Argyropoulou and Papaioannou, 2022; ISPRA et al., 2022), according to which beach macro-litter density reach values up to 230 items/100 m, whereas seafloor macro litter density is equal to 0.7 items/100 m^2 on average.

4. Discussion and conclusions

Besides providing the site-specific findings on macro-plastic transport in the coastal area adjacent to the MPA of Capo Milazzo discussed in Section 3, the present work contributes to the scarce existing literature on the numerical modelling of marine litter trajectories and fates in coastal regions. The velocity field forcing marine plastic displacement in coastal regions is usually generated considering the effects of tidal elevation, and in some cases wind action (Tong et al., 2021; Cloux et al., 2022; Wisha et al., 2022; Cardoso-Mohedano et al., 2023), fluvial flows (Sousa et al., 2021; Cloux et al., 2022; Pilechi et al., 2022), and atmospheric forcing (Sousa et al., 2021; Tong et al., 2021; Cloux et al., 2022; Cardoso-Mohedano et al., 2023). In addition to existing studies, in the present work a wave boundary condition is also imposed, in order to include the wave-induced longshore currents, as well as the effects of the Stokes drift experienced by particles in the direction of wave propagation, which up to now has been considered only in some non-coastal numerical investigations (Liubartseva et al., 2018; Mansui et al., 2020; Baudena et al., 2022; Castro-Rosero et al., 2023; Dobler et al., 2022). The shore-parallel component of the radiation stresses associated with the breaking process approaching the coastline at an oblique angle significantly contributes to the marine plastic transport in coastal areas (Hanes, 2022). In particular, the numerical results obtained for the coastal area adjacent to the MPA of Capo Milazzo presented in Section 3.1 reveal that the wave-induced current velocities reach values of the order of 10^{-1} m/s close to the coast. Moreover, both experimental and numerical studies demonstrated that also the Stokes drift plays a crucial role in floating marine litter transport (Delandmeter and Van Sebille, 2019; Bosi et al., 2021; Calvert et al., 2021; Castro-Rosero et al., 2023). Existing numerical investigation on marine plastic transport in coastal regions mainly focused on floating particles subjected to current advection and turbulent diffusion, in some cases including a parameterization of the beaching processes based on the definition of a constant probability of beaching (Sousa et al., 2021; Cloux et al., 2022) or on the residence time of marine plastic on beach from field measurement

(Wisha et al., 2022). Only Wisha et al. (2022) included the windage effects on buoyant plastic transport, whereas Cardoso-Mohedano et al. (2023) considered the case of non-buoyant plastics subject to a settling velocity calculated using the Stokes' law. In the present work, where both buoyant and non-buoyant macro-plastic are considered, a more comprehensive representation of the process pathways marine plastic items undergo is provided. In particular, besides beaching, which occurs when the particle exits the domain reaching the land, tidal washing-off is also simulated, based on the probabilistic approach described in Section 2.4.2.

The results on marine plastic transport presented in Section 3 should be read considering the limitations due to the modelling choices made in the present work, and in particular that:

- offshore litter sources such as commercial fishery, navigation actions, waste disposal, and shellfish/fish culture (Thushari and Senevirathna, 2020) are not included in the Lagrangian simulations;
- only yearly averaged and extreme hydrodynamic conditions are simulated, considering a statistically significant number of moving particles.

Concerning the choice not to simulate the offshore plastic release, it descends from the scarce available information on the possible location of sea-based litter sources close to the study area, as well as from the modest estimated number (i.e. less than 20 %) of seafloor (Scotti et al., 2021) and beached (Argyropoulou and Papaioannou, 2022; ISPRA et al., 2022) offshore originated plastics at the study site. However, several studies suggested that the assessment of plastic quantities should be done by weight rather than by numbers of items, since this can significantly change the perspective of the contribution of each source type, as well as the pattern of beach loading along the coast (Eriksen et al., 2014; Smith and Turrell, 2021; Allison et al., 2023). This is due to the fact that fishery waste is usually bigger and/or heavier than the land based one. The possible presence of massive litter coming from offshore may be crucial for the optimal beach clean-up planning, and hence the simulation of offshore plastic sources together with the land-based ones could produce interesting outcomes.

Many existing numerical investigations adopted different combinations of multiple plastic sources, also including the sea-based ones. For instance, Lebreton et al. (2012) and Eriksen et al. (2014) took into account three types of plastic sources for the global ocean, which are shipping lanes, rivers, and cities. Similarly, Liubartseva et al. (2018), Soto-Navarro et al. (2020) and Baudena et al. (2022) employed a multiple-source approach to model plastic transport in the Mediterranean Sea. For the Eastern Ionian Sea, Politikos et al. (2020) also included ports and sampling sites as plastic sources. Instead, Guerrini et al. (2021) considered plastic waste released in the Mediterranean Sea by coastal cities, rivers and the most active fishing grounds, thus neglecting the shipping lanes. On the contrary, Critchell et al. (2015) simulated plastic release in the area of the Great Barrier Reef (East coast of Australia) ignoring the contribution of cities and fishery and considering only the inputs from urban rivers and shipping activities. Finally, Ruiz et al. (2022) numerically investigated only the transport of fishing-related floating marine litter in the Bay of Biscay (between France and Spain).

In order to assess the effect of neglecting offshore plastic sources in the final plastic distributions and fates discussed in Section 3, further simulations with three additional seeding points close to the offshore boundary of the domain are run, considering the hydrodynamic condition Winter_01, i.e. winter representative mean wave and wind climate (Table 5) and the case of buoyant (scenario 3: $K_h = 5\ \mathrm{m^2/s}$, beaching/washing-off on, $T_w = 1$ day) and non-buoyant (scenario 10: $K_h = 5\ \mathrm{m^2/s}$, beaching/washing-off on, $T_w = 1$ day; $w_s = 5$ mm/s) macro-plastics. A total of 80 particles are released, equally distributed among the eight seeding points. The results reveal that the offshore-released particles exit the numerical domain or reach the accumulation zones already found in the absence of sea-based sources. Moreover, the proportion between the possible plastic fates including the offshore sources is the same as that found without considering the latter. Therefore, in the present case the decision not to include offshore sources seems not to significantly affect the final outcomes of the plastic transport modelling.

The choice to simulate the transport of a statistically significant number of particles (i.e. from 50 to 5,000 particles) under yearly averaged and extreme hydrodynamic conditions allows the identification of representative plastic pathways and fates in the study area. Other numerical investigations focused on the effects of non-stationary wind and wave fields and river floods, by simulating time series of real hydrodynamic events. For example, a short temporal scale was considered to investigate plastic transport due to circulation patterns typical of particular periods of the year (e.g. Alosairi et al., 2020; Wisha et al., 2022), whereas at least two years were simulated to obtain results on average annual and seasonal marine litter displacement (e.g. Macias et al., 2019; Baudena et al., 2022). Moreover, some existing studies provided realistic quantitative characterization of plastic bulk following two main approaches: i) estimate of the number of particles to be released from cities, rivers and sea-based sources based on empirical relationships between plastic production and quantitative features of the corresponding source, such as population density, economic status of the individual region, index of plastic waste per inhabitant, surface runoff in the watersheds, and daily fishing effort (Guerrini et al., 2021; Tong et al., 2021; Tsiaras et al., 2021; Baudena et al., 2022; Li et al., 2023); ii) release of a statistically significant number of particles and conversion of such a number by applying a correction factor based on the estimate of the annual plastic input in the study area and the average weight of a plastic item (Turrell, 2020; Allison et al., 2022).

Another limitation of the present work is linked to the employment of a 2D velocity field, whereas a 3D hydrodynamic approach would provide a more accurate description of the sinking process (Sousa et al., 2021; Pilechi et al., 2022; Cardoso-Mohedano et al., 2023). The limitations due to the assumptions of the Lagrangian model are mainly due to the fact that shape, size and density of macro-plastics are not accounted for. Moreover, the parameterization of beaching and washing-off processes, and of bed load and bottom particle refloating is still at an early stage of development (Jalòn-Rojas and Marieu, 2023). Finally, the particle hetero- and homo-aggregation, agglomeration, weathering and photodegradation are not considered by any of the existing particle tracking models.

Future numerical investigations on plastic transport in the coastal region of the MPA of Capo Milazzo will focus on the definition of more realistic plastic inputs in terms of location and quantity of produced plastic, based on the results of new monitoring campaigns covering the whole study area. Indeed, the outcomes of the already performed field surveys are not sufficient for a comprehensive characterization of litter that can be found over the investigated beach. Furthermore, time series of real hydrodynamics events will be employed to obtain information about the effects of seasonal circulation patterns. Together with the improvement of plastic sources characterization, this would also enable the accurate validation of the model outputs.

In general, further research is needed for a more comprehensive representation of marine plastic pathways in coastal areas, which should consider a 3D velocity field together with the inclusion of degradation of macro-plastic and biofouling. Moreover, the parameterization of the beaching and washing-off processes should be improved in order to take into account the combined effects of tides, waves, and winds, also considering the peculiarity of the coastline and the possible presence of trapping structures such as groins and breakwaters.

CRediT authorship contribution statement

M. Stagnitti: Writing – original draft, Validation, Methodology, Investigation, Formal analysis. **R.E. Musumeci:** Writing – review & editing, Validation, Supervision, Methodology, Formal analysis,

Conceptualization.

Declaration of competing interest

The authors declare that they have no known competing financial interests or personal relationships that could have appeared to influence the work reported in this paper.

Data availability

Data will be made available on request.

Acknowledgments

The authors would like to thank the Department of Biomedical Science and Bio-technologies (BIOMETEC) of the University of Catania for participating to the filed survey and performing the laboratory analyses. Moreover, this work has been funded by: the project BIOBLU (J49C20000060007), financed by the European Fund for Regional Development in ten context of the program INTERREG Italia-Malta 2014-2020; the project PLATONE (2022BCJ5W3), financed by the PRIN fund in the context of the PNRR; the project VARIO, financed by the program PIACERI of the University of Catania; the project REST-COAST (101037097), financed by Horizon 2020 European Union Funding for Research & Innovation; the project ISYPORT (ARS01_01202) in the framework of PNR 2015-2020.

References

Alfonso, M.B., Arias, A.H., Menéndez, M.C., Ronda, A.C., Harte, A., Piccolo, M.C., Marcovecchio, J.E., 2021. Assessing threats, regulations, and strategies to abate plastic pollution in lac beaches during covid-19 pandemic. Ocean Coast. Manag. 208, 105613.

Allison, N.L., Dale, A., Turrell, W.R., Aleynik, D., Narayanaswamy, B.E., 2022. Simulating the distribution of beached litter on the northwest coast of Scotland. Front. Environ. Sci. 10, 940892.

Allison, N.L., Dale, A.C., Turrell, W.R., Narayanaswamy, B.E., 2023. Modelled and observed plastic pollution on remote Scottish beaches: the importance of local marine sources. Mar. Pollut. Bull. 194, 115341.

Alomar, C., Deudero, S., 2017. Evidence of microplastic ingestion in the shark galeus melas- tomus rafinesque, 1810 in the continental shelf off the Western Mediterranean Sea. Environ. Pollut. 223, 223–229.

Alosairi, Y., Al-Salem, S., Al Ragum, A., 2020. Three-dimensional numerical modelling of transport, fate and distribution of microplastics in the Northwestern Arabian/Persian Gulf. Mar. Pollut. Bull. 161, 111723.

Al-Salem, S., Alosairi, Y., Constantinou, A., 2022. Effect of covid-19 lockdown measures on the plastic waste generation trends and distribution of microplastics in the Northwestern Arabian/Persian Gulf. Ocean Coast. Manag. 216, 105979.

Alsina, J.M., Jongedijk, C.E., van Sebille, E., 2020. Laboratory measurements of the wave-induced motion of plastic particles: influence of wave period, plastic size and plastic density. J. Geophys. Res. Oceans 125, e2020JC016294.

Angiolillo, M., Fortibuoni, T., Di Lorenzo, B., Tunesi, L., 2023. First baseline assessment of seafloor litter on Italian coralligenous assemblages (Mediterranean Sea) in accordance with the European Marine Strategy Framework Directive. Mar. Pollut. Bull. 187, 114597.

Argyropoulou, K., Papaioannou, I., 2022. Plastic busters MPAs - final conference report (deliverable 6.4.5). The Interreg MED plastic busters MPAs project, plasticbusters-mpas.Interreg-med.Eu.

Asensio-Montesinos, F., Anfuso, G., Williams, A.T., Sanz-Lázaro, C., 2021. Litter behaviour on Mediterranean cobble beaches, SE Spain. Mar. Pollut. Bull. 173, 113106.

Balbar, A.C., Metaxas, A., 2019. The current application of ecological connectivity in the design of marine protected areas. Global Ecology and Conservation 17, e00569.

Baudena, A., Ser-Giacomi, E., Jalón-Rojas, I., Galgani, F., Pedrotti, M.L., 2022. The streaming of plastic in the Mediterranean Sea. Nat. Commun. 13, 1–9.

Bigdeli, M., Mohammadian, A., Pilechi, A., Taheri, M., 2022. Lagrangian modeling of marine microplastics fate and transport: the state of the science. Journal of Marine Science and Engineering 10, 481.

Boccotti, P., 2004. Idraulica marittima. UTET Università.

Booij, N., Ris, R.C., Holthuijsen, L.H., 1999. A third-generation wave model for coastal regions: 1. Model description and validation. J. Geophys. Res. Oceans 104, 7649–7666.

Bosi, S., Broström, G., Roquet, F., 2021. The role of stokes drift in the dispersal of North Atlantic surface marine debris. Front. Mar. Sci. 8, 697430.

Brouwer, R., Huang, Y., Huizenga, T., Frantzi, S., Le, T., Sandler, J., Dijkstra, H., van Beukering, P., Costa, E., Garaventa, F., et al., 2023. Assessing the performance of marine plastics cleanup technologies in Europe and North America. Ocean Coast. Manag. 238, 106555.

Calvert, R., McAllister, M., Whittaker, C., Raby, A., Borthwick, A., Van Den Bremer, T., 2021. A mechanism for the increased wave-induced drift of floating marine litter. J. Fluid Mech. 915, A73.

Campana, I., Angeletti, D., Crosti, R., Di Miccoli, V., Arcangeli, A., 2018. Seasonal patterns of floating macro-litter across the Western Mediterranean Sea: a potential threat for cetacean species. Rendiconti Lincei. Scienze Fisiche e Naturali 29, 453–467.

Campanale, C., Suaria, G., Bagnuolo, G., Baini, M., Galli, M., De Rysky, E., Ballini, M., Aliani, S., Fossi, M.C., Uricchio, V.F., 2019. Visual observations of floating macro litter around Italy (mediterranean sea). Mediterr. Mar. Sci. 20, 271–281.

Camus, P., Haigh, I.D., Wahl, T., Nasr, A.A., Méndez, F.J., Darby, S.E., Nicholls, R.J., 2022. Daily synoptic conditions associated with occurrences of compound events in estuaries along North Atlantic coastlines. Int. J. Climatol. 42, 5694–5713.

Cardoso, C., Caldeira, R.M., 2021. Modeling the exposure of the Macaronesia Islands (NE Atlantic) to marine plastic pollution. Front. Mar. Sci. 8, 653502.

Cardoso-Mohedano, J.G., Ruiz-Fernández, A.C., Sanchez-Cabeza, J.A., Camacho-Torres, S.M., Ontiveros-Cuadras, J.F., 2023. Microplastics transport in a low-inflow estuary at the entrance of the gulf of California. Sci. Total Environ. 870, 161825.

Carlson, D.F., Suaria, G., Aliani, S., Fredj, E., Fortibuoni, T., Griffa, A., Russo, A., Melli, V., 2017. Combining litter observations with a regional ocean model to identify sources and sinks of floating debris in a semi-enclosed basin: the Adriatic Sea. Front. Mar. Sci. 4, 78.

Castro-Rosero, L.M., Hernandez, I., Alsina, J.M., Espino, M., 2023. Transport and accumulation of floating marine litter in the Black Sea: insights from numerical modeling. Front. Mar. Sci. 10, 1213333.

Chassignet, E.P., Xu, X., Zavala-Romero, O., 2021. Tracking marine litter with a global ocean model: where does it go? Where does it come from? Front. Mar. Sci. 8, 667591.

Chubarenko, I., Bagaev, A., Zobkov, M., Esiukova, E., 2016. On some physical and dynamical properties of microplastic particles in marine environment. Mar. Pollut. Bull. 108, 105–112.

Claro, F., Fossi, M.C., Ioakeimidis, C., Baini, M., Lusher, A.L., Mc Fee, W., McIntosh, R.R., Pelamatti, T., Sorce, M., Galgani, F., et al., 2019. Tools and constraints in monitoring interactions between marine litter and megafauna: insights from case studies around the world. Mar. Pollut. Bull. 141, 147–160.

Cloux, S., Allen-Perkins, S., de Pablo, H., Garaboa-Paz, D., Montero, P., Muñuzuri, V.P., 2022. Validation of a lagrangian model for large-scale macroplastic tracer transport using mussel-peg in NW Spain (Ría de Arousa). Sci. Total Environ. 822, 153338.

Consoli, P., Falautano, M., Sinopoli, M., Perzia, P., Canese, S., Esposito, V., Battaglia, P., Romeo, T., Andaloro, F., Galgani, F., et al., 2018. Composition and abundance of benthic marine litter in a coastal area of the central Mediterranean Sea. Mar. Pollut. Bull. 136, 243–247.

Coppock, R.L., Galloway, T.S., Cole, M., Fileman, E.S., Queirós, A.M., Lindeque, P.K., 2019. Microplastics alter feeding selectivity and faecal density in the copepod, calanus helgolandicus. Sci. Total Environ. 687, 780–789.

Corbau, C., Lazarou, A., Buoninsegni, J., Olivo, E., Gazale, V., Nardin, W., Simeoni, U., Carboni, D., 2023. Linking marine litter accumulation and beach user perceptions on pocket beaches of Northern Sardinia (Italy). Ocean Coast. Manag. 232, 106442.

Critchell, K., Lambrechts, J., 2016. Modelling accumulation of marine plastics in the coastal zone; what are the dominant physical processes? Estuar. Coast. Shelf Sci. 171, 111–122.

Critchell, K., Grech, A., Schlaefer, J., Andutta, F., Lambrechts, J., Wolanski, E., Hamann, M., 2015. Modelling the fate of marine debris along a complex shoreline: lessons from the Great Barrier Reef. Estuar. Coast. Shelf Sci. 167, 414–426.

Cui, T., Kamath, A., Wang, W., Han, D., Bihs, H., 2022. Large-eddy simulations of gravity currents in the presence of waves. J. Hydraul. Res. 60, 770–791.

De Leo, A., Cutroneo, L., Sous, D., Stocchino, A., 2021. Settling velocity of microplastics exposed to wave action. Journal of Marine Science and Engineering 9, 142.

Delandmeter, P., Van Sebille, E., 2019. The parcels v2. 0 lagrangian framework: new field interpolation schemes. Geosci. Model Dev. 12, 3571–3584.

Deltares, 2021a. D-flow flexible mesh. Computational cores and user Interface. User Manual. Technical Report. Boussinesqweg 1, 2629 (HV Delft, P.O. 177, 2600 MH Delft, The Netherlands).

Deltares, 2021b. D-waves flexible mesh. Simulation of short-crested waves with SWAN. User Manual. Technical Report. Boussinesqweg 1, 2629 (HV Delft, P.O. 177, 2600 MH Delft, The Netherlands).

Deltares, 2021c. RGFGRID. Generation and manipulation of structured and unstructured grids, suitable for Delft3D-FLOW, Delft3DWAVE or D-FLOW flexible mesh. User Manual. Technical Report. Boussinesqweg 1, 2629 (HV Delft, P.O. 177, 2600 MH Delft, The Netherlands).

Diaconu, C., Şerban, P., 1994. Sinteze şi regionalizări hidrologice. Editura Tehnică, Bucarest.

DiBenedetto, M.H., Clark, L.K., Pujara, N., 2022. Enhanced settling and dispersion of inertial particles in surface waves. J. Fluid Mech. 936, A38.

Dobler, D., Maes, C., Martinez, E., Rahmania, R., Gautama, B.G., Farhan, A.R., Dounias, E., 2022. On the fate of floating marine debris carried to the sea through the main rivers of Indonesia. Journal of Marine Science and Engineering 10, 1009.

Eriksen, M., Lebreton, L.C., Carson, H.S., Thiel, M., Moore, C.J., Borerro, J.C., Galgani, F., Ryan, P.G., Reisser, J., 2014. Plastic pollution in the world's oceans: more than 5 trillion plastic pieces weighing over 250,000 tons afloat at sea. PLoS One 9, e111913.

European Commission, 2013. Guidance on monitoring of marine litter in European seas. A guidance document within the common implementation strategy for the marine strategy framework directive. Technical report. MSFD technical subgroup on marine litter, Luxembourg, publications Office of the European Union.

Feng, Q., Chen, Z., Greer, C.W., An, C., Wang, Z., 2022. Transport of microplastics in shore substrates over tidal cycles: roles of polymer characteristics and environmental factors. Environ. Sci. Technol. 56, 8187–8196.
Fossi, M.C., Vlachogianni, T., Galgani, F., Degli Innocenti, F., Zampetti, G., Leone, G., 2020. Assessing and mitigating the harmful effects of plastic pollution: the collective multi-stakeholder driven Euro-Mediterranean response. Ocean Coast. Manag. 184, 105005.
Galli, M., Baini, M., Panti, C., Giani, D., Caliani, I., Campani, T., Rosso, M., Tepsich, P., Levati, V., Laface, F., et al., 2023. Oceanographic and anthropogenic variables driving marine litter distribution in Mediterranean protected areas: extensive field data supported by forecasting modelling. Sci. Total Environ. 903, 166266.
Garcia-Garin, O., Borrell, A., Aguilar, A., Cardona, L., Vighi, M., 2020. Floating marine macro-litter in the North Western Mediterranean Sea: results from a combined monitoring approach. Mar. Pollut. Bull. 159, 111467.
González-Fernández, D., Hanke, G., 2020. Monitoring approaches for marine litter in the european sea basins. In: Plastics in the Aquatic Environment-Part II: Stakeholders' Role against Pollution. Springer, pp. 139–156.
Google Earth. Coastal region adjiacent ot the Marine Protected Area of Capo Milazzo, Sicily, Italy. 38.1595°N, 15.17779°E, Eye alt 27.96 km. http://www.earth.google.com.
Guerrini, F., Mari, L., Casagrandi, R., 2021. The dynamics of microplastics and associated contaminants: data-driven lagrangian and eulerian modelling approaches in the Mediterranean Sea. Sci. Total Environ. 777, 145944.
Hanes, D.M., 2022. Longshore currents. In: Treatise on Geomorphology, 2nd Edition. Academic Press, Oxford, pp. 83–99. https://doi.org/10.1016/B978-0-12-818234-5.00051-1. Chapter 8.04.
Hersbach, H., Bell, B., Berrisford, P., Biavati, G., Horányi, A., Muñoz Sabater, J., Nicolas, J., Peubey, C., Radu, R., Rozum, I., et al., 2018. Era5 hourly data on single levels from 1979 to present. Copernicus climate change service (c3s) climate data store (cds) 10. https://doi.org/10.24381/cds.adbb2d47.
Hinata, H., Sagawa, N., Kataoka, T., Takeoka, H., 2020. Numerical modeling of the beach process of marine plastics: a probabilistic and diagnostic approach with a particle tracking method. Mar. Pollut. Bull. 152, 110910.
Interreg Europe, 2021. Halting Ocean Plastics Pollution. A Policy Brief for the Policy Learning Platform on Environment and Resource Efficiency. Technical Report. European Union. European Regional Development Found.
Isobe, A., Kako, S., Chang, P.H., Matsuno, T., 2009. Two-way particle-tracking model for specifying sources of drifting objects: application to the East China Sea shelf. J. Atmos. Ocean. Technol. 26, 1672–1682.
ISPRA, Stazione Zoologica Anton Dohrn (AP), Università di Siena, Consorzio AMP Capo Milazzo, 2022. The plastic busters mpas marine litter monitoring results and achieve- ments at Capo Milazzo (Italy). https://mio-ecsde.org/wp-content/uploads/2022/04/PBM_CAPITALIZATION-CONFERENCE_Athens_S3_P03_Angiolillo.pdf.
Iwasaki, S., Isobe, A., Kako, S., Uchida, K., Tokai, T., 2017. Fate of microplastics and meso- plastics carried by surface currents and wind waves: a numerical model approach in the sea of Japan. Mar. Pollut. Bull. 121, 85–96.
Jalòn-Rojas, I., Marieu, V., 2023. Tutorial. trackmpd v2.3.
Jalón-Rojas, I., Wang, X.H., Fredj, E., 2019. A 3d numerical model to track marine plastic debris (TrackMPD): sensitivity of microplastic trajectories and fates to particle dynamical properties and physical processes. Mar. Pollut. Bull. 141, 256–272.
Kako, S., Isobe, A., Kataoka, T., Hinata, H., 2014. A decadal prediction of the quantity of plastic marine debris littered on beaches of the East Asian marginal seas. Mar. Pollut. Bull. 81, 174–184.
Kiran, B.R., Kopperi, H., Venkata Mohan, S., 2022. Micro/nano-plastics occurrence, identification, risk analysis and mitigation: challenges and perspectives. Rev. Environ. Sci. Biotechnol. 21, 169–203.
Kirpich, Z., 1940. Time of concentration of small agricultural watersheds. Civ. Eng. 10, 362.
Klink, D., Peytavin, A., Lebreton, L., 2022. Size dependent transport of floating plastics modeled in the global ocean. Front. Mar. Sci. 9, 903134.
Korres, G., Ravdas, M., Zacharioudaki, A., Denaxa, D., Sotiropoulou, M., 2021. Mediterranean Sea waves reanalysis (cmems med-waves, medwam3 system) (version 1) data set. Copernicus Monitoring Environment Marine Service (CMEMS). https://doi.org/10.25423/CMCC/MEDSEA_MULTIYEAR_WAV_006_012.
Kowalski, N., Reichardt, A.M., Waniek, J.J., 2016. Sinking rates of microplastics and potential implications of their alteration by physical, biological, and chemical factors. Mar. Pollut. Bull. 109, 310–319.
Lebreton, L., Andrady, A., 2019. Future scenarios of global plastic waste generation and disposal. Palgrave Communications 5, 1–11.
Lebreton, L.M., Greer, S., Borrero, J.C., 2012. Numerical modelling of floating debris in the world's oceans. Mar. Pollut. Bull. 64, 653–661.
Lee, M.K.K., 2021. Plastic pollution mitigation–net plastic circularity through a standardized credit system in asia. Ocean Coast. Manag. 210, 105733.
Li, Y., Wolanski, E., Dai, Z., Lambrechts, J., Tang, C., Zhang, H., 2018. Trapping of plastics in semi-enclosed seas: insights from the Bohai Sea, China. Mar. Pollut. Bull. 137, 509–517.
Li, Y., Yu, H., Qin, Y.H., Guo, K.X., Yang, Y.Q., Zhang, M.Y., Lu, W., Zhang, Y., 2023. Numerical simulation research of the transportation and distribution characteristics on sea surface of the microplastic released continuously for 12 years from China's coastal cities. Mar. Environ. Res. 190, 106100.
Liu, Y., Weisberg, R.H., 2011. Evaluation of trajectory modeling in different dynamic regions using normalized cumulative lagrangian separation. J. Geophys. Res. Oceans 116.
Liu, Y., Weisberg, R.H., Vignudelli, S., Mitchum, G.T., 2014. Evaluation of altimetry-derived surface current products using lagrangian drifter trajectories in the eastern Gulf of Mexico. J. Geophys. Res. Oceans 119, 2827–2842.
Liubartseva, S., Coppini, G., Lecci, R., Clementi, E., 2018. Tracking plastics in the Mediterranean: 2D lagrangian model. Mar. Pollut. Bull. 129, 151–162.
Lots, F.A., Behrens, P., Vijver, M.G., Horton, A.A., Bosker, T., 2017. A large-scale investigation of microplastic contamination: abundance and characteristics of microplastics in European beach sediment. Mar. Pollut. Bull. 123, 219–226.
Macias, D., Cózar, A., Garcia-Gorriz, E., González-Fernández, D., Stips, A., 2019. Surface water circulation develops seasonally changing patterns of floating litter accumulation in the Mediterranean Sea. A modelling approach. Mar. Pollut. Bull. 149, 110619.
Macias, D., Stips, A., Hanke, G., 2022. Model based estimate of transboundary litter pollution on mediterranean coasts. Mar. Pollut. Bull. 175, 113121.
Maestro, M., Pérez-Cayeiro, M.L., Chica-Ruiz, J.A., Reyes, H., 2019. Marine protected areas in the 21st century: current situation and trends. Ocean Coast. Manag. 171, 28–36.
Mandić, M., Gvozdenović, S., De Vito, D., Alfonso, G., Daja, S., Ago, B., Cela, E., Ivanović, A., Zoto, A., Malovrazić, N., et al., 2022. Setting thresholds is not enough: beach litter as indicator of poor environmental status in the southern Adriatic Sea. Mar. Pollut. Bull. 177, 113551.
Mansui, J., Darmon, G., Ballerini, T., Van Canneyt, O., Ourmieres, Y., Miaud, C., 2020. Predicting marine litter accumulation patterns in the Mediterranean basin: spatio-temporal variability and comparison with empirical data. Prog. Oceanogr. 182, 102268.
Marino, M., Stagnitti, M., Stancanelli, L.M., Musumeci, R.E., Foti, E., 2023. Dynamics of wave-supported gravity currents in intermediate water. Cont. Shelf Res. 267 (1050), 82.
Menicagli, V., De Battisti, D., Balestri, E., Federigi, I., Maltagliati, F., Verani, M., Castelli, A., Carducci, A., Lardicci, C., 2022. Impact of storms and proximity to entry points on marine litter and wrack accumulation along Mediterranean beaches: management implications. Sci. Total Environ. 824, 153914.
Murawski, J., She, J., Frishfelds, V., 2022. Modeling drift and fate of microplastics in the Baltic Sea. Front. Mar. Sci. 9, 886295.
Musumeci, R.E., Viviano, A., Foti, E., 2017. Influence of regular surface waves on the propagation of gravity currents: experimental and numerical modeling. J. Hydraul. Eng. 143, 04017022.
Nielsen, P., 1992. Coastal Bottom Boundary Layers and Sediment Transport, 4. World scientific.
Nunes, B.Z., Huang, Y., Ribeiro, V.V., Wu, S., Holbech, H., Moreira, L.B., Xu, E.G., Castro, I.B., 2022. Microplastic contamination in seawater across global marine protected areas boundaries. Environ. Pollut. 316, 120692.
Onink, V., Kaandorp, M.L., van Sebille, E., Laufk'øtter, C., 2022. Influence of particle size and fragmentation on large-scale microplastic transport in the Mediterranean Sea. Environ. Sci. Technol. 56, 15528–15540.
P.A.I, 2004a. Piano Stralcio di Bacino per l'Assetto Idrogeologico del Torrente Mazzarà (010). Technical Report, Regione Siciliana, Italy.
P.A.I, 2004b. Piano Stralcio di Bacino per l'Assetto Idrogeologico del Torrente Mela (010). Technical Report, Regione Siciliana, Italy.
P.A.I, 2004c. Piano Stralcio di Bacino per l'Assetto Idrogeologico del Torrente Termini ed area compresa tra i bacini del torrente Termini e del Mazzarà (010). Technical Report, Regione Siciliana, Italy.
Passalacqua, G., Iuppa, C., Faraci, C., 2023. A simplified experimental method to estimate the transport of non-buoyant plastic particles due to waves by 2D image processing. Journal of Marine Science and Engineering 11, 1599.
Peng, L., Fu, D., Qi, H., Lan, C.Q., Yu, H., Ge, C., 2020. Micro-and nano-plastics in marine environment: source, distribution and threats—a review. Sci. Total Environ. 698, 134254.
Peng, Y., Wu, P., Schartup, A.T., Zhang, Y., 2021. Plastic waste release caused by covid-19 and its fate in the global ocean. Proc. Natl. Acad. Sci. 118 (e2111), 530118.
Pilechi, A., Mohammadian, A., Murphy, E., 2022. A numerical framework for modeling fate and transport of microplastics in inland and coastal waters. Mar. Pollut. Bull. 184, 114119.
Poeta, G., Battisti, C., Bazzichetto, M., Acosta, A.T., 2016. The cotton buds beach: marine litter assessment along the Tyrrhenian coast of Central Italy following the Marine Strategy Framework Directive criteria. Mar. Pollut. Bull. 113, 266–270.
Politikos, D., Tsiaras, K., Papatheodorou, G., Anastasopoulou, A., 2020. Modeling of floating marine litter originated from the Eastern Ionian Sea: transport, residence time and connectivity. Mar. Pollut. Bull. 150, 110727.
PRCEC, 2020. Piano Regionale Contro l'Erosione Costiera. Versione 2.0. Technical Report.. Regione Siciliana, Italy.
Prevenios, M., Zeri, C., Tsangaris, C., Liubartseva, S., Fakiris, E., Papatheodorou, G., 2018. Beach litter dynamics on Mediterranean coasts: distinguishing sources and pathways. Mar. Pollut. Bull. 129, 448–457.
Robinson, T., Eames, I., Simons, R., 2013. Dense gravity currents moving beneath progressive free-surface water waves. J. Fluid Mech. 725, 588–610.
Röhrs, J., Christensen, K.H., Hole, L.R., Broström, G., Drivdal, M., Sundby, S., 2012. Observa- tion-based evaluation of surface wave effects on currents and trajectory forecasts. Ocean Dyn. 62, 1519–1533.
Rosas, E., Martins, F., Tosic, M., Janeiro, J., Mendonça, F., Mills, L., 2022. Pathways and hot spots of floating and submerged microplastics in Atlantic Iberian marine waters: a modelling approach. Journal of Marine Science and Engineering 10, 1640.
Ruiz, I., Basurko, O.C., Rubio, A., et al., 2022. Modelling the distribution of fishing-related floating marine litter within the bay of Biscay and its marine protected areas. Environ. Pollut. 292, 118216.
Saladié, Ò., Bustamante, E., 2021. Abundance and composition of marine litter on the seafloor of the gulf of sant jordi (western mediterranean sea). Environments 8, 106.

Sayol, J.M., Orfila, A., Simarro, G., Conti, D., Renault, L., Molcard, A., 2014. A lagrangian model for tracking surface spills and Sar operations in the ocean. Environ. Model Softw. 52, 74–82.
Scotti, G., Esposito, V., D'Alessandro, M., Panti, C., Vivona, P., Consoli, P., Figurella, F., Romeo, T., 2021. Seafloor litter along the Italian coastal zone: an integrated approach to identify sources of marine litter. Waste Manag. 124, 203–212.
Shen, M., Ye, S., Zeng, G., Zhang, Y., Xing, L., Tang, W., Wen, X., Liu, S., 2020. Can microplastics pose a threat to ocean carbon sequestration? Mar. Pollut. Bull. 150, 110712.
Smith, L., Turrell, W.R., 2021. Monitoring plastic beach litter by number or by weight: the implications of fragmentation. Front. Mar. Sci. 8, 702570.
Soares, J., Miguel, I., Venâncio, C., Lopes, I., Oliveira, M., 2020. Perspectives on micro (nano) plastics in the marine environment: biological and societal considerations. Water 12, 3208.
Soto-Navarro, J., Jordá, G., Deudero, S., Alomar, C., Amores, Á., Compa, M., 2020. 3D hotspots of marine litter in the Mediterranean: a modeling study. Mar. Pollut. Bull. 155, 111159.
Sousa, M.C., DeCastro, M., Gago, J., Ribeiro, A.S., Des, M., Gómez-Gesteira, J.L., Dias, J. M., Gomez-Gesteira, M., 2021. Modelling the distribution of microplastics released by wastewater treatment plants in Ria de Vigo (NW Iberian peninsula). Mar. Pollut. Bull. 166, 112227.
Spedicato, M.T., Walter, Z., Pierluigi, C., Fabio, F., Follesa, M.C., François, G., Cristina, G. R., Angélique, J., Christos, I., Giorgos, L., et al., 2019. Spatial distribution of marine macro-litter on the seafloor in the Northern Mediterranean Sea: the MEDITS initiative. Sci. Mar. 83, 257–270.
Stancanelli, L., Musumeci, R., Foti, E., 2018a. Dynamics of gravity currents in the presence of surface waves. J. Geophys. Res. Oceans 123, 2254–2273.
Stancanelli, L.M., Musumeci, R.E., Foti, E., 2018b. Computational fluid dynamics for modeling gravity currents in the presence of oscillatory ambient flow. Water 10, 635.
Svendsen, I.A., 2005. Introduction to Nearshore Hydrodynamics, 24. World Scientific Publishing Company.
Thompson, R.C., Olsen, Y., Mitchell, R.P., Davis, A., Rowland, S.J., John, A.W., McGonigle, D., Russell, A.E., 2004. Lost at sea: where is all the plastic? Science 304, 838.
Thushari, G.G.N., Senevirathna, J.D.M., 2020. Plastic pollution in the marine environment. Heliyon 6.
Tong, X., Jong, M.C., Zhang, J., You, L., Gin, K.Y.H., 2021. Modelling the spatial and seasonal distribution, fate and transport of floating plastics in tropical coastal waters. J. Hazard. Mater. 414, 125502.
Tsiaras, K., Hatzonikolakis, Y., Kalaroni, S., Pollani, A., Triantafyllou, G., 2021. Modeling the pathways and accumulation patterns of micro-and macro-plastics in the Mediterranean. Front. Mar. Sci. 1389.
Turrell, W., 2020. Estimating a regional budget of marine plastic litter in order to advise on marine management measures. Mar. Pollut. Bull. 150, 110725.
UNEP-WCMC, IUCN, 2021. Protected Planet Report 2020. Technical Report. UNEP-WCMC and IUCN:. Cambridge UK, Gland, Switzerland.
Uzun, P., Farazande, S., Guven, B., 2022. Mathematical modeling of microplastic abundance, distribution, and transport in water environments: a review. Chemosphere 288, 132517.
Valente, T., Pelamatti, T., Avio, C.G., Camedda, A., Costantini, M.L., de Lucia, G.A., Jacomini, C., Piermarini, R., Regoli, F., Sbrana, A., et al., 2022. One is not enough: monitoring microplastic ingestion by fish needs a multispecies approach. Mar. Pollut. Bull. 184, 114133.
Van Sebille, E., Aliani, S., Law, K.L., Maximenko, N., Alsina, J.M., Bagaev, A., Bergmann, M., Chapron, B., Chubarenko, I., Cózar, A., et al., 2020. The physical oceanography of the transport of floating marine debris. Environ. Res. Lett. 15, 023003.
Viviano, A., Musumeci, R.E., Foti, E., 2018. Interaction between waves and gravity currents: description of turbulence in a simple numerical model. Environ. Fluid Mech. 18, 117–148.
Vlachogianni, T., Fortibuoni, T., Ronchi, F., Zeri, C., Mazziotti, C., Tutman, P., Varezić, D.B., Palatinus, A., Trdan, Š., Peterlin, M., et al., 2018. Marine litter on the beaches of the Adriatic and Ionian seas: an assessment of their abundance, composition and sources. Mar. Pollut. Bull. 131, 745–756.
Wang, B., Yang, R., Fang, Q., 2023. Marine plastic management policy agenda-setting in China (1985–2021): the multi-stage streams framework. Ocean Coast. Manag. 243, 106761.
Wang, E., Miao, C., Chen, X., 2022. Circular economy and the changing geography of inter- national trade in plastic waste. Int. J. Environ. Res. Public Health 19, 15020.
Wilson, K.L., Tittensor, D.P., Worm, B., Lotze, H.K., 2020. Incorporating climate change adaptation into marine protected area planning. Glob. Chang. Biol. 26, 3251–3267.
Wisha, U.J., Gemilang, W.A., Wijaya, Y.J., Purwanto, A.D., 2022. Model-based estimation of plastic debris accumulation in Banten bay, Indonesia, using particle tracking-flow model hydrodynamics approach. Ocean Coast. Manag. 217, 106009.
Xu, K., Ma, C., Lian, J., Bin, L., 2014. Joint probability analysis of extreme precipitation and storm tide in a coastal city under changing environment. PLoS One 9, e109341.
Zayen, A., Sayadi, S., Chevalier, C., Boukthir, M., Ismail, S.B., Tedetti, M., 2020. Microplastics in surface waters of the gulf of Gabes, southern mediterranean sea: distribution, composition and influence of hydrodynamics. Estuar. Coast. Shelf Sci. 242 (1068), 32.
Zeri, C., Adamopoulou, A., Varezić, D.B., Fortibuoni, T., Viršek, M.K., Kržan, A., Mandic, M., Mazziotti, C., Palatinus, A., Peterlin, M., et al., 2018. Floating plastics in Adriatic waters (Mediterranean Sea): from the macro-to the micro-scale. Mar. Pollut. Bull. 136, 341–350.
Zheng, F., Westra, S., Sisson, S.A., 2013. Quantifying the dependence between extreme rainfall and storm surge in the coastal zone. J. Hydrol. 505, 172–187.